Int. J. Heat Mass Transfer. Vol. 6, pp. 363–385. Pergamon Press 1963. Printed in Great Britain.

MASS TRANSFER THROUGH LAMINAR BOUNDARY LAYERS—4. CLASS I METHODS FOR PREDICTING MASS-TRANSFER RATES

D. B. SPALDING† and S. W. CHI‡

Mechanical Engineering Department, Imperial College of Science and Technology, London, S.W.7

(*Received* 6 *November* 1962)

Abstract—Exact solutions of the uniform-property laminar-boundary-layer equations, presented in earlier papers of the series, are used in developing approximate methods for predicting mass-transfer rates from two-dimensional and axi-symmetrical surfaces with arbitrary main-stream velocity when the interface and transferred-substance conditions are uniform along the surface. The mass-transfer rate is obtained sufficiently accurately for many purposes from the evaluation of a single quadrature involving the main-stream velocity and constants which depend on the Prandtl/Schmidt number; an iterative procedure is presented which increases the accuracy somewhat. The method is a development of that of Eckert and Livingood, and makes use of the quadrature procedure of Walz.

NOMENCLATURE

b, dimensionless flux property, equation (2);
b_0', gradient of b adjacent to the interface, equation (A1) and Paper 3;
B, dimensionless driving force, equation (1);
c, constant-pressure specific heat of mass stream, Btu/lb degF, footnote Section 2.3;
c_{cool}, constant-pressure specific heat of coolant, Btu/lb degF, footnote Section 2.3;
E_4, correction factor for F_4, equation (39);
F_4, equal to $(u_G/\nu)\,(d\Delta_4^2/dx)$, equation (39);
f_0, dimensionless stream function at interface, Appendix (A);
f_0'', dimensionless velocity gradient at interface, Appendix (A);
$\mathbf{G}$, total mass-flux vector, lb/ft² h, equation (2);
g, surface conductance for mass transfer, lb/ft² h, equation (1);
I, integral of equation (51), Paper 3;
J, K, coefficients in equation (51), Paper 3;
l, cylinder diameter or sphere diameter, ft, Figs. 14, 17;
L, reference length, ft, equation (21);
m, mass fraction of a substance, equation (5);
$m_{O,G}$, mass fraction of oxygen in main stream, equation (54);
$\dot{m}''$, mass-transfer rate per unit area, lb/ft² h, equation (1);
n_c, mass of carbon per unit mass of steel, equation (54);
P, conserved property, equation (4);
p, q, see equation (40) and Fig. 7;
R, distance of point on surface from axis of symmetry, ft, equation (26);
R_0, reference radius, ft, equation (26);
g_0, constant in Newton's second law of motion, lb ft/lbf h², equation (52);
t, temperature, degF, footnote Section 2.3;
r_i, mass of oxygen which combines with unit mass of iron, equation (54);
u, flow velocity in x-direction, ft/h;
u_G, u in main stream, ft/h, equation (6);
U, flow velocity approaching cylinder or sphere, ft/h, equation (20);
v, flow velocity in y-direction, ft/h;
v_S, v at surface, ft/h, equation (7);
x, distance measured along wall in same direction as mainstream, ft, equation (6);

† Professor of Heat Transfer.
‡ Research Student.

y, perpendicular distance from wall, ft, equation (3);
z, distance perpendicular to x and y, ft, Table 1.

Greek symbols

β, a constant related to pressure gradient, equation (6);
δ_2, momentum thickness, ft, equation (7);
Δ_2, convective thickness, equation (18);
Δ_4, conductive thickness, equation (6);
γ, exchange coefficient, lb/ft h, equation (2);
μ, dynamic viscosity, lb/ft h, equation (15);
ν, kinematic viscosity, ft²/h, equation (6);
ρ, density, lb/ft³, equation (8);
σ, Prandtl or Schmidt number, equation (6);
τ_S, shear stress at wall, lbf/ft², equation (52).

Subscripts and Superscripts

G, main-stream state, equation (4);
S, state adjacent interface, equation (4);
T, state of transferred substance, equation (4);
0, axi-symmetrical stagnation point, equation (32);
*, non-dimensional quantities defined by equations (20–22);
**, non-dimensional quantities defined by equations (25–27);
I, 1st approximation, equation (42);
II, 2nd approximation, equation (43);
III, 3rd approximation, equation (51).

INTRODUCTION

1.1. *Purpose of the paper*

THE PRESENT paper is the fourth of a series, intended to provide methods for predicting rates of mass transfer through laminar forced convection uniform-property boundary layers. Papers 1 and 2, [1, 2] were devoted to methods of calculating the properties of the velocity boundary layer when the mass-transfer rate is specified. Paper 3, [3] considered the "similar" solutions of the differential equation for the distribution of a conserved property; it therefore dealt with problems of the standard mass-transfer type, but was restricted to simple geometrical circumstances.

In the present paper we turn to the general problem: the prediction of mass-transfer rates without restriction as to free-stream velocity distribution. The method to be presented here is not the most general or most accurate; but it probably possesses the most useful combination of accuracy, ease of use and range of validity of all those currently available. A more accurate and generally valid method will be presented in Paper 5 of the series; this will be found however to involve appreciably greater computational difficulty than the present one.

1.2. *The problem to be solved*

Expressed in physical terms. We consider a surface of prescribed shape, immersed in a fluid stream (Fig. 1). We suppose that the

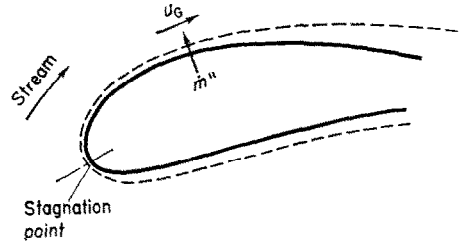

FIG. 1. Illustrating the problem of calculating mass-transfer rates.

velocity of the stream outside a relatively thin boundary layer, u_G, is given for all points on the surface. In addition, we postulate knowledge of the values of at least one conserved fluid property (e.g. enthalpy, or mass fraction of an inert chemical compound) for three fluid states: that of the main stream (G), that of the fluid adjacent the surface (S), and that of the substance transferred into the stream (T). The problem is to determine the rate (e.g. in lb/ft² h) at which material is transferred across the prescribed surface into (or, of course, out of) the main stream. This quantity will be denoted by $\dot{m}''$.

In order to give geometrical significance to some of the important quantities, it is customary to define, and to focus attention on, certain

"boundary-layer thicknesses", to which the mass-transfer flux is directly related. The problem then becomes that of predicting the appropriate thickness of the boundary layer at all points of the surface.

Our problem arises in connexion with many natural and technological processes, including: drying of wet material in an air stream; combustion of a liquid fuel; dissolution of a salt in a liquid stream; "ablation" of the nose-cone of a space-vehicle re-entering the earth's atmosphere; condensation of steam on a cold surface; and many others.

Expressed in mathematical terms, the formulation which will be adopted is that of reference [4], where it was shown that the mass-transfer rate can be expressed as a product of a conductance g, and a dimensionless driving force B; thus:

$$\dot{m}'' = g \, . \, B. \tag{1}$$

Further, the conductance is obtained from the solution of a partial differential equation by evaluating the gradient of a potential b at the surface. The equation is:

$$\mathbf{G} \, . \, (\nabla b) - \nabla[\gamma(\nabla b)] = 0 \tag{2}$$

where $\mathbf{G}$ is the total mass-flux vector (lb/ft² h), b is the dimensionless fluid property (potential), equal to zero at the interface engaging in mass transfer, and equal to B in the main stream. γ is an exchange coefficient (lb/ft h), equal to a diffusion coefficient times the fluid density, or to the thermal conductivity divided by the specific heat, according to the nature of the conserved property for which b stands.

The relation between the conductance and the gradient at the interface is:

$$g = \left(\gamma \frac{\partial b}{\partial y}\right)_S / B \tag{3}$$

where y is distance normal to the interface, suffix S stands for fluid conditions adjacent the interface.

The driving force B is obtained by evaluation of a suitable thermodynamic property, P, for the fluid in the main stream (G-state), at the interface (S-state) and in the transferred substance (T-state). The appropriate general relation is:

$$B \equiv \frac{P_G - P_S}{P_S - P_T}. \tag{4}$$

For example, if water is vaporizing into (or condensing from) an air stream, an appropriate form of the driving force would be:

$$B = \frac{m_{H_2O,\,G} - m_{H_2O,\,S}}{m_{H_2O,\,S} - 1} \tag{5}$$

where m_{H_2O} is the mass of steam per unit mass of local mixture (lb/lb) and $m_{H_2O,\,T} = 1$, since the transferred substance consists entirely of H_2O. Other examples of the driving force B will be found in [4]. In the present paper, however, B can be regarded as a quantity whose value is known: our task is to find means of evaluating g.

The mathematical expression of the problem dealt with in the present paper is thus: find the solution to (2) for the geometry and flow conditions illustrated in Fig. 1, taking the G-distribution from the relevant solution of the equation of motion; then deduce g via (3), and $\dot{m}''$ via (1).

Restrictions on the scope of the inquiry are as in earlier papers of the series. The flow is supposed to be steady and laminar, and of sufficiently high Reynolds number for a boundary layer to form; the transport properties and the density of the fluid are supposed uniform; the geometry of the surface is such that the flow is either two-dimensional or axi-symmetrical; and the main stream can be regarded as large in extent so that all its thermodynamic properties, P_G, are uniform outside the boundary layer.

In addition, the method of the present paper is restricted to situations in which the relevant properties of the fluid at the surface and in the transferred substance, P_S and P_T, are uniform over the surface.

1.3. *Classification of methods*

Except for those situations which give rise to the "similar" boundary layers dealt with in Paper 3, equation (2) is rarely solved exactly; for it is a partial differential equation, requiring numerical solution. Although the equation degenerates, in a boundary-layer situation, from

an elliptic to a parabolic form, and so becomes amenable to forward integration, the computational labour is still prohibitive as a rule.

Approximate methods of solution are therefore used. These have mostly been developed to deal with heat transfer in the absence of mass transfer; this means that they provide approximate solutions to (2) for the particular case in which B tends to zero. However the methods can be made to apply to non-zero values of B also, as will be seen.

The methods are of two classes, designated I and II in [5], but have one common feature: the assumption, either implicit or explicit, that all the profiles of velocity and of thermodynamic properties (P or b) appearing in the boundary layer belong to a restricted family. This assumption results in the reduction of parabolic differential equations to ordinary ones.

The two classes of methods are distinguished by the number of differential equations which have to be solved.† Methods of Class I involve consideration of only one differential equation; this may be either the (degenerate form of) equation (2), as in the methods of Eckert [6] and Smith and Spalding [5]; or it may be the (degenerate form of the) velocity equation as in the methods of Seban [7] and of Drake [8]. In the latter case it is necessary to assume *explicitly* that the boundary layers of velocity and of b at any location bear the same relation to each other as they do in the corresponding "similar" flows of Paper 3; in the former case, this assumption is made *implicitly*.

Methods of Class II involve the solution of differential equations for both the velocity and the b-boundary layers. They therefore involve more computational labour than do the Class I methods. When mass transfer is absent ($B \to 0$), the b-equation can be solved *after* solution of the velocity equation; this has been the case in all methods of this class which have been developed hitherto [9, 10, 11, 12]. When mass transfer is present, on the other hand, the two equations must be solved *simultaneously*.

The present paper provides Class I methods for the prediction of mass-transfer rates. The greater part of the attention will be devoted to a method of the Eckert type (solution of the b-equation); however a method of the Seban–Drake type (solution of the u-equation) will also be discussed.

Eckert and Livingood [15] have already extended the method of [6] to problems of mass transfer, in the particular context of transpiration cooling. The present paper builds on their foundation and makes the following extensions: (i) greater range of parameters, including negative B, large positive B and a wide range of σ-values, (ii) greater accuracy of auxiliary functions, obtained by use of exact solutions of the boundary-layer equations not available to the earlier authors, (iii) more direct derivation of the equations by the use of vectorial dimensional analysis, (iv) application of Walz's [16] quadrature procedure for solving the differential equation, and presentation of the necessary constants, (v) improvements to Walz's procedure, enabling second and higher approximations to be obtained.

1.4. *Outline of the present paper*

Section 2 presents the extension of the Seban–Drake method to the calculation of mass transfer. It is presented first since it is rather directly related to the procedures introduced in Paper 1 of the series, and forms a convenient introduction to the somewhat more subtle method of Section 3, namely the extended Eckert method. Because the Seban–Drake section is not the recommended one, Section 2 appears in small print.

The development of the argument is similar to that followed in Paper 1; it has the following steps: simplifying assumption, dimensional analysis, reference to the "similar" solutions for the form of functions appearing in an ordinary differential equation, provision of a quadrature procedure, and extension to axi-symmetrical flows. The most useful formula resulting from this discussion is equation (44); combined with the auxiliary Tables 4a and 4b, this equation is all that is needed by readers solely concerned

† If this system of classification is accepted, we ought to introduce a Class Zero for methods in which *no* differential equations are solved; such methods, which were omitted from the listing of Smith and Spalding [5] are exemplified by the method of Stine and Wanlass [13], which is discussed later (footnote to Section 3.1). Numerous heat-transfer methods have been classified in this way in [14].

with the use of the method. For many purposes the first approximation, equation (45), is sufficiently accurate.

Section 4 provides some examples of the use of the method of Section 3.

2. EXTENSION OF THE SEBAN–DRAKE METHOD TO MASS TRANSFER

2.1. *The argument*

The "similar" solutions of the *b*-equation [equation (2)], which were discussed in Paper 3, could be represented in the form:

$$\frac{\Delta_4^2}{\nu}\frac{\mathrm{d}u_G}{\mathrm{d}x} = f(\beta, B, \sigma). \tag{6}$$

Here Δ_4 = "conduction thickness" (ft)
$= \gamma/g = B/(\partial b/\partial y)_S$,
ν = kinematic viscosity of fluid (ft²/h),
β = dimensionless quantity relating to pressure gradient,
σ $= \mu/\gamma$ = Prandtl or Schmidt number (dimensionless),
μ = dynamic viscosity of fluid (lb/ft h),
$f(\ldots)$ = "some function of . . .".

The "similar" solutions of the velocity equation, which were discussed in Papers 1 and 2 of the series, could be put in the form:

$$\frac{\delta_2^2}{\nu}\frac{\mathrm{d}u_G}{\mathrm{d}x} = f\left(\beta, \frac{v_S\delta_2}{\nu}\right). \tag{7}$$

Here δ_2 = "momentum thickness" (ft)
$= \int_0^\infty (u/u_G)[1 - (u/u_G)]\,\mathrm{d}y$,
v_S = normal velocity at the surface (ft/h)
$= \dot{m}''/\rho$,
ρ = fluid density (lb/ft³),
$f(\ldots)$ = "some function of . . .", of course not the same function as that of equation (6).

Now the definitions of Δ_4, g and v_S imply the relations:

$$B = \frac{\rho v_S \Delta_4}{\gamma} = \frac{v_S\delta_2}{\nu}\cdot\frac{\Delta_4}{\delta_2}\cdot\frac{\mu}{\gamma}. \tag{8}$$

Consequently, β can be eliminated between (6) and (7), and the resulting relation can be cast in the form:

$$\boxed{\frac{\Delta_4}{\delta_2} = f\left(\frac{\delta_2^2}{\nu}\frac{\mathrm{d}u_G}{\mathrm{d}x}, B, \sigma\right)} \tag{9}$$

where $f(\ldots)$ of course now stands for yet another function.

The essential assumption. Equation (9) is exact only for a restricted family of flows: we shall take the "similar-solution" family, when establishing the form of the function. However, all the quantities appearing in the equation are *local* i.e. measurable at a particular location on the surface; no knowledge is required of distance from the leading edge, for example. It is therefore clear that an approximate method for predicting Δ_4 can be developed if we make the *assumption*: equation (9) shall be regarded as valid for "non-similar" as well as for "similar" boundary layers.

The method. Paper 1 has already explained how δ_2 can be calculated, in a given flow, by solution of the differential equation:

$$\frac{u_G}{\nu}\frac{\mathrm{d}\delta_2^2}{\mathrm{d}x} = F_2\left(\frac{\delta_2^2}{\nu}\frac{\mathrm{d}u_G}{\mathrm{d}x}, \frac{v_S\delta_2}{\nu}\right). \tag{10}$$

Since v_S is not a given quantity in problems of the type considered here, while B is, we introduce (8) and (9) into (10); this then takes the more useful form:

$$\frac{u_G}{\nu}\frac{\mathrm{d}\delta_2^2}{\mathrm{d}x} = F_2\left(\frac{\delta_2^2}{\nu}\frac{\mathrm{d}u_G}{\mathrm{d}x}, B, \sigma\right). \tag{11}$$

Provided the function F_2, the constants ν, B, and the velocity distribution $u_G(x)$ are known, equation (11) can be solved numerically: the result is a distribution of δ_2 over the surface. Paper 1 presented some techniques for doing this, and some examples.

Once $\delta_2(x)$ is given, $\Delta_4(x)$ can be obtained via equation (9), provided of course that the function appearing there is tabulated.

2.2. *Auxiliary functions*

Papers 1 and 2 contain graphs and tables of (u_G/ν) $(\mathrm{d}\delta_2^2/\mathrm{d}x)$ as a function of (δ_2^2/ν) $(\mathrm{d}u_G/\mathrm{d}x)$ and $v_S\delta_2/\nu$. To use these in the above method it is simply necessary to have a means of evaluating $v_S\delta_2/\nu$ for each value of B, σ and (δ_2^2/ν) $(\mathrm{d}u_G/\mathrm{d}x)$. The method will be illustrated by means of the following example.

2.3. *Use of the method*

As an illustration, we consider a transpiration-cooling problem. We suppose that a surface has to be cooled by forcing a gas through the surface, which is made porous for this purpose. Specification of the stream, coolant and desired surface temperatures fixes the driving force B; let us suppose that this has the value 1·0 in the present case.† Suppose further that the free-stream velocity distribution is given, e.g. via Fig. 2 which happens to be valid, according to Schmidt and Wenner [17], for a cylinder.

Here U is the approach velocity and l is the cylinder diameter. Assuming the Prandtl number σ to be 0·7, and taking $B = 1{\cdot}0$, we can find a value of $v_S\delta_2/\nu$ for each

† The relation is: $B = c(t_G - t_S)/c_{cool}\,(t_S - t_T)$ in the absence of radiation, where t_G, t_T and t_S are respectively the temperatures referred to in the text, while c and c_{cool} are respectively the constant-pressure specific heats of the main stream and of the coolant. For explanation, see [4].

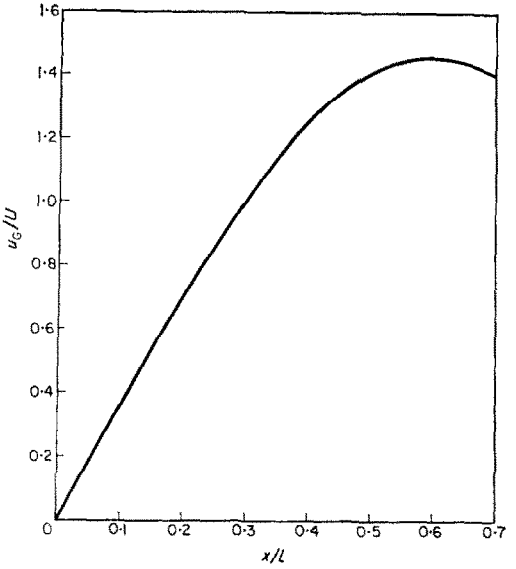

FIG. 2. Velocity distribution, $u_G(x)$, for the front half of a cylinder [17].

value of $(\delta_2^2/\nu)\,(du_G/dx)$ from the "similar" solutions of Papers 1, 2, and 3. This set of values defines a line on Fig. 3, which is taken from Paper 1 of the series and represents the auxiliary function F_2; the curve corresponding to $\sigma = 0{\cdot}7$ and $B = 1{\cdot}0$ is the one marked "exact" on Fig. 3.

The existence of this curve permits us to write equation (10) as:

$$\frac{u_G}{\nu}\frac{d\delta_2^2}{dx} = F_2\left(\frac{\delta_2^2}{\nu}\frac{du_G}{dx}\right) \tag{12}$$

which can now be solved numerically since δ_2^2 is the only unknown. However an approximate solution is obtainable more easily if the curve is replaced by a straight line as also shown in Fig. 3; in the present case, this approximation may be represented by re-writing (12) as:

$$\frac{u_G}{\nu}\frac{d\delta_2^2}{dx} = 0{\cdot}6725 - 5{\cdot}87\,\frac{\delta_2^2}{\nu}\frac{du_G}{dx} \tag{13}$$

which has the closed-form solution:

$$\delta_2 = \left(\frac{0{\cdot}6725\nu}{u_G^{5{\cdot}87}}\int_0^x u_G^{4{\cdot}87}\,dx\right)^{1/2}. \tag{14}$$

Once δ_2 has been evaluated at points of interest by inserting the given $u_G(x)$ function in the quadrature of (14), the quantities Δ_4, g or $\dot{m}''$ are easily obtained from the similar solutions. Thus, if the mass-transfer rate $\dot{m}''$ is required, we simply recall that, from the definitions:

$$\dot{m}'' = \rho v_S = \frac{\mu}{\delta_2}\cdot\frac{v_S\delta_2}{\nu} \tag{15}$$

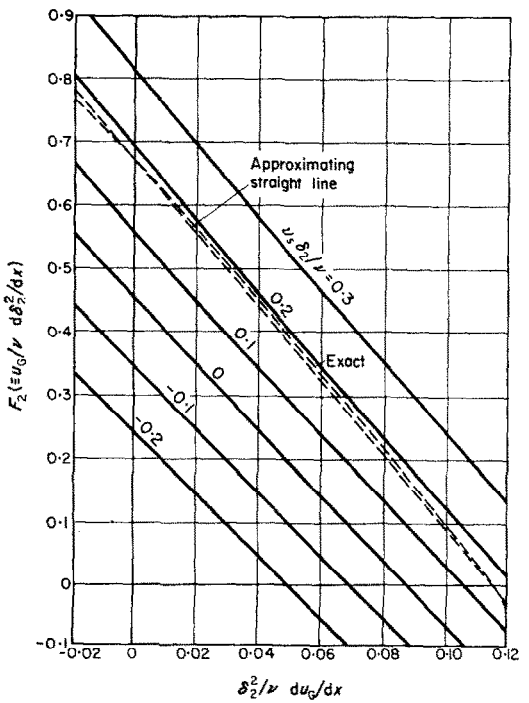

FIG. 3. F_2 vs. $(\delta_2^2/\nu)(du_G/dx)$ with $v_S\delta_2/\nu$ as parameter. Broken lines are for $B = 1{\cdot}0$ and $\sigma = 0{\cdot}7$.

Now the value of $v_S\delta_2/\nu$ can be obtained, for each value of $(\delta_2^2/\nu)\,du_G/dx$, directly from Fig. 3: it lies close to 0·18 in the present example. The right-hand side of (15) can therefore be deduced from the δ_2 (x) values yielded by (14). Fig. 4 shows the results, for the present example, in the form of curves of $(\delta_2/l)\,(Ul/\nu)^{1/2}$ and of $(\dot{m}''\,l/\mu)\,(Ul/\nu)^{1/2}$ versus x/l. Two pairs of curves are exhibited, one based on the exact F_2-functions, the other based on the linear approximation of equation (13); the difference between the two solutions is seen to be negligible for most purposes.

2.4. *Discussion*

The method just described has the advantage that it is merely a modification and extension of that presented in Paper 1 for the approximate prediction of the properties of the velocity layer; it therefore provides no new conceptual difficulties.

On the other hand, the use of the method requires the availability of two sets of auxiliary functions: those of Paper 1 and those contained in Paper 3.

Another aspect of the same disadvantage is that, in carrying out the calculation, we are

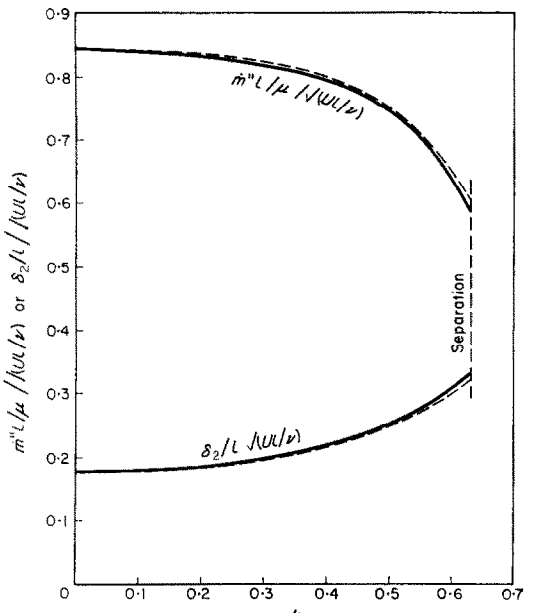

FIG. 4. Solution for transpiration cooling of a cylinder with $B = 1$, $\sigma = 0{\cdot}7$ by method of Section 2. Dotted line using linear approximation for F_2. Solid line using exact values of F_2.

forced to evaluate properties of the *velocity* boundary layer in which we are not directly interested.†

In these circumstances it is reasonable to ask: "Why not eliminate reference to δ_2 by postulating the existence of a differential equation like (11) but with Δ_4^2 as the independent variable?" The recognition of this question, and the elaboration of its implications, are to be credited to Eckert [6], who was there solely concerned with heat transfer ($B = 0$). The same author subsequently explored the case $B \neq 0$ [15]; we here follow in his footsteps, taking also the opportunity to display the logic of the method more completely than has been customary.

3. EXTENSION OF THE ECKERT METHOD TO MASS TRANSFER

3.1. *The argument*

Simplifying assumption. Focusing attention on the "conduction thickness" Δ_4, we now ask ourselves what the rate of growth of Δ_4 can depend on. If we postulate the same "shortness of memory" which was supposed, in Paper 1, to characterize the velocity boundary layer, we can allow only *local* properties to appear in the answer to this question. We thus suppose that $d\Delta_4/dx$ depends only on: u_G, du_G/dx, $\dot{m}''$, Δ_4, δ_2, ν, ρ, γ, B. The distance x from the start of the boundary layer is specifically excluded from this list since we argue that this is not a local property and that the boundary layer should have no "recollection" of it.‡

Dimensional analysis. We now apply a dimensional analysis, in which account is taken of the laminar boundary-layer simplification which ensures that viscous and diffusive effects are responsive only to gradients in the y-direction (normal to the wall). In this case the x-, and y-, and z-directions may be regarded as possessing different dimensions (viz. X, Y, Z). The dimensions of all the quantities appearing in the previous paragraph are therefore as shown in Table 1, where T stands for the dimension of time and M stands for the dimension of mass. It will be noted that nine physical quantities appear in the table, and that there are four independently appearing dimensions (X, Y, T and M/Z); we deduce that the physical quantities are related by an equation involving five (i.e. nine minus four) dimensionless quantities. These might conveniently be:

$$\frac{u_G}{\nu}\frac{d\Delta_4^2}{dx}, \quad \frac{\Delta_4^2}{\nu}\frac{du_G}{dx}, \quad \frac{\Delta_4}{\delta_2}, \quad \frac{\dot{m}''\Delta_4}{\gamma}, \quad \frac{\rho\nu}{\gamma}.$$

† Of course, if we *are* interested in calculating how much effect the mass transfer has on the drag coefficient, etc. this remark does not apply.

‡ It is in this respect that the method, like that of Paper 1 of the series, differs from the Class-Zero method of Stine and Wanlass [13], for example. The latter authors eliminate $d\Delta_4/dx$ from the functional relationship and substitute x. This implies that the boundary layer has a highly selective memory: it can recollect how far it is from the stagnation point, but forgets everything that has happened between that point and the local station. Although it must be admitted that no definitive comparison of the relative accuracy of the Class-Zero and Class I methods has ever been made, the unreasonableness of the assumption has influenced the authors to pay relatively little attention to Class-Zero methods in the present work. Although these methods simplify computation (the disappearance of $d\Delta_4/dx$ means that there is no longer a differential equation to be solved) the authors believe that this is at the expense of physical plausibility.

Table 1

Quantity	$d\Delta_4/dx$	u_G	du_G/dx	$\dot{m}''$	Δ_4	δ_2	ν	ρ	γ
Dimensions	Y/X	X/T	$1/T$	M/XZT	Y	Y	Y^2/T	M/XYZ	MY/XZT

The last two dimensionless groups appearing in this list are respectively equal to B and to σ, by reason of previously introduced definitions.

Differential equations for boundary-layer growth. It follows that the simplifying assumption noted at the beginning of this section can be expressed symbolically as:

$$\frac{u_G}{\nu}\frac{d\Delta_4^2}{dx} = F_4\left(\frac{\Delta_4^2}{\nu}\frac{du_G}{dx}, \frac{\Delta_4}{\delta_2}, B, \sigma\right) \qquad (16)$$

where F_4 is an as-yet-unknown function.

As in the method of Paper 1, we can determine the form of the function $F_4(\ldots.)$ by reference to the "similar" solutions. If this is done straightforwardly, however, it is found that the function has only three independent arguments; for the four quantities appearing in $F_4(\ldots.)$ are already linked via (9). This fact permits us to drop the quantity Δ_4/δ_2 and to reduce equation (16) to:

$$\frac{u_G}{\nu}\frac{d\Delta_4^2}{dx} = F_4\left(\frac{\Delta_4^2}{\nu}\frac{du_G}{dx}, B, \sigma\right). \qquad (17)$$

Equation (17) is the differential equation for growth of the conduction thickness Δ_4. It does not contain the momentum thickness δ_2 explicitly. It may be solved by numerical means whenever $u_G(x)$ is specified and B and σ are known.

Discussion. The argument which has just been developed in terms of Δ_4 could equally well have been applied to the convection thickness Δ_2, defined by:

$$\Delta_2 \equiv \int_0^\infty u_G\left(1 - \frac{b}{B}\right)dy. \qquad (18)$$

If this had been done, the equation corresponding to (17) would have been the "integral b-conservation" equation, namely:

$$\frac{1}{2}\frac{u_G}{\nu}\frac{d\Delta_2^2}{dx} = \frac{(1+B)}{\sigma}\frac{\Delta_2}{\Delta_4} - \frac{\Delta_2^2}{\nu}\frac{du_G}{dx}. \qquad (19)$$

The procedure for solving (19) is the same as that for (17); in this case it is necessary to express $[(1 + B)/\sigma]\,(\Delta_2/\Delta_4)$ as a function of $(\Delta_2^2/\nu)\,(du_G/dx)$ by reference to the "similar" solutions. Equation (19) is therefore no easier to solve than (17); and its solution still involves the assumption that local conditions are identical with those in "similar" boundary layers. Nevertheless, solutions to (19) may be regarded as more satisfactory (i.e. likely to correspond with reality) than those to (17); for at least equation (19) is derived directly from the rigorous partial differential equations, whereas equation (17) is not.

Despite this consideration, the use of Δ_4 is preferable as a rule because the mass-transfer rate may be determined from it directly. The use of Δ_4 rather than Δ_2 is a particularly bold extension of the line of thought underlying the so-called "integral methods", first developed in connection with the velocity boundary layer; there however only δ_2 is considered as a variable. The extension was first made by Eckert [6].

Another reason for preferring Δ_4 to Δ_2 has been uncovered in [5]; considering only the case of $B = 0$, the authors of this reference showed that the Δ_2-equation is less amenable to approximate solution as a quadrature than is the Δ_4 equation. This is of course not a consideration to which weight need be given by those who are well equipped for the numerical solution of non-linear differential equations.

3.2. *The prediction procedure*

We are now in a position to describe a procedure for predicting the mass-transfer rate at any point on a surface for which B, σ and $u_G(x)$ are specified, in the form of the following list of instructions:

Step (i) Choose reference values of velocity, U, and length L; these may conveniently be the velocity far upstream of the body and the

overall length along the surface of the body, but other choices are permissible and may sometimes be desirable.

Step (ii) Define non-dimensional quantities u_G^*, x^*, and Δ_4^* as follows:

$$u_G^* \equiv u_G/U \tag{20}$$

$$x^* \equiv x/L \tag{21}$$

$$\Delta_4^* \equiv \Delta_4 \sqrt{(U/L\nu)}. \tag{22}$$

The differential equation to be solved now becomes

$$u_G^* \frac{d\Delta_4^{*2}}{dx^*} = F_4\left(\Delta_4^{*2} \frac{du_G^*}{dx^*}, B, \sigma\right). \tag{23}$$

Step (iii) Differentiate the u_G^* (x^*) curve appropriate to the particular problem, so that now du_G^*/dx^* and u_G^* are both available as functions of x^*.

Step (iv) Solve equation (23) by standard procedures of numerical analysis (e.g. Runge-Kutta) referring to Step (iii) for the functions particular to the problem, and to a general table or graph of F_4 for the particular values of B and σ in question. Note that Δ_4^{*2} (du_G^*/dx^*) is identical in value with (Δ_4^2/ν) (du_G/dx).

The result of this step is a curve of Δ_4^* versus x^*.

Step (v) Evaluate $\dot{m}''$ at each value of x^* from the relation:

$$\dot{m}'' = \frac{\gamma B}{\Delta_4^*} \sqrt{\left(\frac{U}{L\nu}\right)}. \tag{24}$$

The auxiliary function F_4. To permit the performance of Step (iv) of the procedure, a table or graph of F_4 is needed. This can be constructed from the similar solutions of the b-equation as explained in Paper 3.

Since the function F_4 has three arguments, the establishment of sufficient tables is a formidable

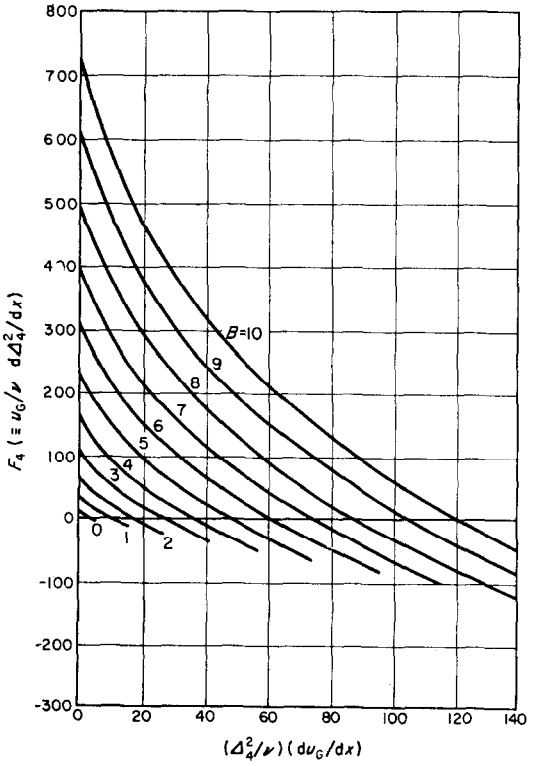

FIG. 5a. F_4 vs. $(\Delta_4^2/\nu)(du_G/dx)$ for $\sigma = 0{\cdot}7$ with B ($\geqslant 0$) as parameter.

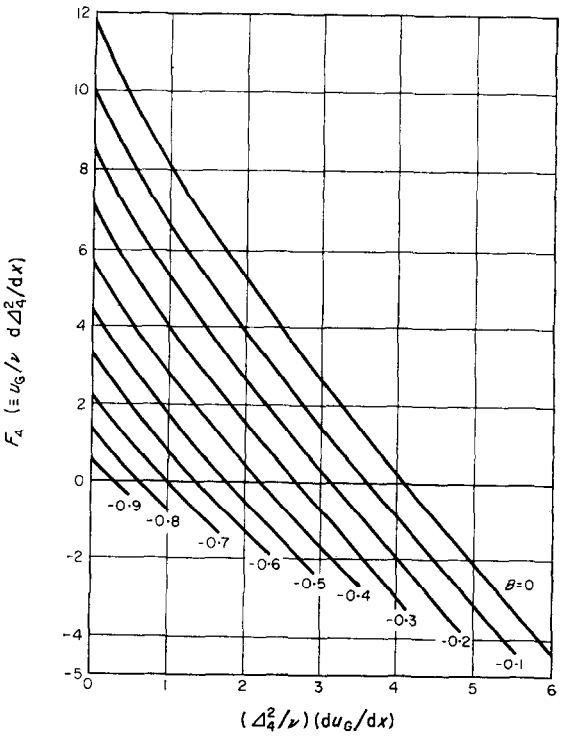

FIG. 5b. F_4 vs. $(\Delta_4^2/\nu)(du_G/dx)$ for $\sigma = 0{\cdot}7$ with B ($\leqslant 0$) as parameter.

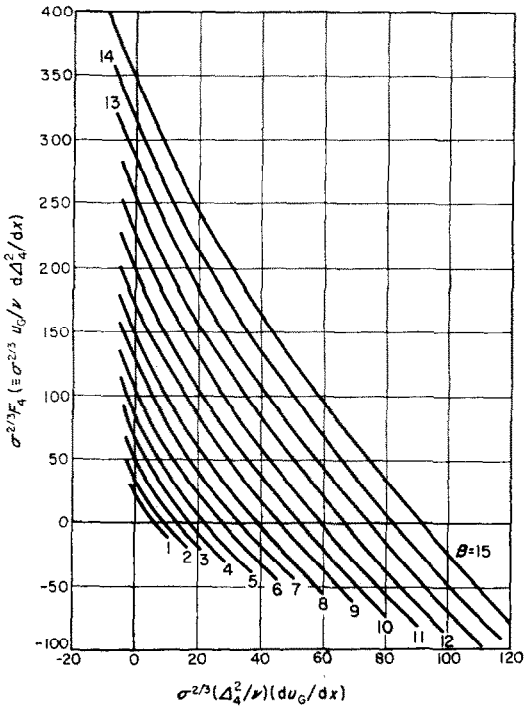

FIG. 6a. $\sigma^{2/3}F_4$ vs. $\sigma^{2/3}(\Delta_4^2/\nu)(\mathrm{d}u_G/\mathrm{d}x)$ for $\sigma \to \infty$ and various B ($\geqslant 0$).

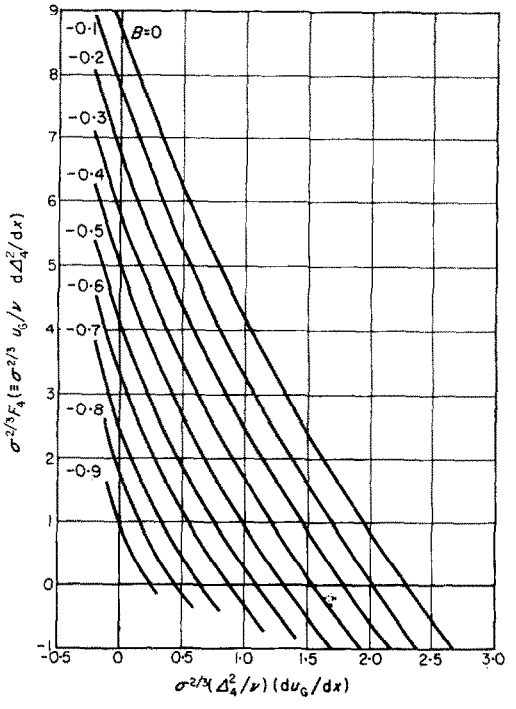

FIG. 6b. $\sigma^{2/3}F_4$ vs. $\sigma^{2/3}(\Delta_4^2/\nu)(\mathrm{d}u_G/\mathrm{d}x)$ for $\sigma \to \infty$ and various B ($\leqslant 0$).

task. In the present paper only two tables are presented; both based on the work reported in Paper 3. Table 2 contains values of F_4 valid for various values of (Δ_4^2/ν) $(\mathrm{d}u_G/\mathrm{d}x)$ and B and for a σ-value of 0·7; the values have been taken almost directly from Paper 3. Table 3 contains values of the quantity $\sigma^{2/3}F_4$ for various values of $\sigma^{2/3}$ (Δ_4^2/ν) $(\mathrm{d}u_G/\mathrm{d}x)$ and B, which are asymptotically correct for high values of σ; the Table has been constructed by the methods outlined in Appendix A.

The contents of Tables 2 and 3 are presented graphically in Figs. 4a, b and a, 5b, it should be noted that, because of the nature of the underlying solutions, Table 2 and Fig. 5 are subject to future amendment as more exact solution of the "similar" b-equation become available; Table 3 and Fig. 6, on the other hand, probably already possess three-figure accuracy

The range of validity of Table 3 and Fig. 6 can be estimated by evaluating F_4 for $\sigma = 0{\cdot}7$ and comparing the values with those in Table 2. Some results of doing so are shown in Table 6. It is seen that although the values from the two tables agree tolerably for $\beta = 0$ and $B = 0$ considerable errors may arise elsewhere. Clearly the use of Table 3 should be restricted to values of σ greater than 0·7.

3.3. *Modification for axi-symmetrical flows*†

It has been shown in Paper 1 of the series that a transformation introduced by Mangler [18] permits problems with axi-symmetrical geometry to be transformed into equivalent two-dimensional problems. Although the proof given in Paper 1 related solely to the momentum equation, it applies to the b-equation (2) with equal force.

As a consequence, the procedure of the last section should be modified, in order to predict mass-transfer rates in axi-symmetrical systems, to:

Step (i) As above. Choose also a reference radius R_0.

† Sections 3.3 and 3.4 are so similar in spirit to the corresponding sections of Paper 1 as to be unnecessary for reasonably expert readers. They have been included here, in small print, for the use of readers who are concerned with the practical use of the method but not so familiar with boundary-layer theory as to be able to work out the steps for themselves in a short time.

Table 2a. F_4 vs. B and $(\Delta_4^3/\nu)(\mathrm{d}u_G/\mathrm{d}x)$ for $\sigma = 0{\cdot}7$ and $B \geqslant 0$

B \ $(\Delta_4^3/\nu)\frac{\mathrm{d}u_G}{\mathrm{d}x}$	0	1	2	3	4	5	6	7	8	9	10	15	20	25	30	40	50	60	70	80	90	100	110	120	130	140
0	11·7	8·08	5·15	2·59	0·209	−2·10																				
0·5	22·1	17·15	13·5	10·40	7·55	5·00	2·54	0·2	−1·97																	
1	34·0	28·4	24·2	20·6	17·4	14·3	11·45	8·57	5·82	3·2	0·66															
1·5	49·2	43·0	37·6	33·1	29·2	25·7	22·5	19·43	16·35	13·38	10·46	−3·0														
2	65·7	59·1	53·3	48·2	43·5	39·5	35·7	32·2	28·7	25·4	22·3	6·70	−5·8													
2·5	86·5	79·4	73·0	67·6	62·3	57·7	53·3	49·0	44·8	40·6	37·1	20·1	5·45	−7·60												
3	110·0	102·7	96·2	90·6	83·3	77·7	72·1	67·0	62·2	58·0	54·0	36·0	19·4	4·90	−8·30											
3·5	135·1	126·7	118·8	111·7	105·3	99·1	93·1	87·4	82·0	76·7	72·0	52·3	35	18·8	3·85	−21										
4	164·0	155·0	146·0	138·4	131·0	124·0	117·6	111·5	105·7	100·2	94·9	73·0	54·1	36·3	19·8	−8·5	−34									
4·5	195·5	185·9	177	168·2	160·2	152·8	145·3	138·7	132	125·9	120	94·8	74·9	56·5	38	5·9	−21·5	−43·7								
5	230	219·6	210	200·5	192·1	183·9	176·2	168·9	162·1	155·6	149	120	97·4	77·9	58·8	25	−4·8	−29·9								
5·5	266	254·7	244·6	235	226	217·4	209·1	201	193·4	186	179	147·3	121·8	100	80·2	45	11·5	−1·8	−41·5							
6	309	297	286	275	265	255	246	237	228	220	212	178	150·8	130·5	117	65·1	31·1	1·5	−24·5	−46·2						
6·5	352	339	327	316	305·5	295	285	276	267	258	250	213·3	181·3	153·8	130·2	89	53·8	21·8	9	−34·9						
7	398	384	372	360	349	339	329	319	310	301	292	251·8	217	186	159	115·6	78·4	41·8	11·2	−16·8	−40·8					
7·5	446	432	419	407·5	395	384·5	374	364	354	344·5	336	293·5	255	222	194·5	144·1	102·7	66·8	33·4	3·1	−2·5	−49·9				
8	497·5	482	469	457	446	434	423	412	401·5	393	383	337·2	296	260	229·1	175·0	130·4	92·8	57·1	25	−4·2	−30·5	−54			
8·5	551	535	521·5	509	496	485	473	461	450	441	432	382	337	299	265	209·8	164·6	124·8	87·6	53	20	−10·3	−35·2			
9	610	593	579	565·5	553	540	527	514	504	492	481·5	428	379·5	339	303	242·5	195	153·5	114·6	78·5	45	12·5	−17	−42		
9·5	671	653·5	638	624	610	596	582	570	555	542·5	530	475	424	381	345	280	229·5	186	144·8	105·0	70·1	31·2	−7·1	−12·2	−46·5	
10	730	711	695	680	665	650	635·5	622	608	595	581	525	474	429	388·6	321·8	256	217·2	173·4	133·6	97	61	30·2	0	−25·2	−49·2

Table 2b. F_4 vs. B and $(\Delta_4^3/\nu)(\mathrm{d}u_G/\mathrm{d}x)$ for $\sigma = 0{\cdot}7$ and $B \leqslant 0$

B \ $(\Delta_4^3/\nu)\frac{\mathrm{d}u_G}{\mathrm{d}x}$	0	0·05	0·1	0·15	0·2	0·3	0·4	0·5	0·6	0·8	1·0	1·2	1·4	1·6	1·8	2·0	2·2	2·4	2·6	2·8	3·0	3·5	4·0	4·5	5·0
0	11·7	11·48	11·25	11·02	10·85	10·45	1·007	9·710	9·383	8·719	8·080	7·450	6·862	6·275	5·70	5·15	4·61	4·08	3·57	3·08	2·59	1·390	0·209	−0·978	−2·10
−0·05	10·85	10·64	10·42	10·24	10·04	9·662	9·313	8·968	8·632	7·987	7·363	6·756	6·170	5·600	5·05	4·51	3·99	3·48	2·99	2·50	2·01	0·824	−0·36	−1·492	
−0·1	9·98	9·78	9·58	9·39	9·19	8·85	8·52	8·19	7·87	7·24	6·62	6·02	5·45	4·89	4·36	3·84	3·34	2·84	2·35	1·87	1·390	0·212	−0·951	−2·06	
−0·15	9·21	8·99	8·80	8·62	8·45	8·11	7·78	7·46	7·14	6·53	5·93	5·35	4·80	4·26	3·74	3·24	2·73	2·25	1·762	1·295	0·827	−0·311	−1·480		
−0·2	8·41	8·23	8·05	7·88	7·71	7·37	7·05	6·74	6·43	5·83	5·25	4·69	4·16	3·65	3·15	2·65	2·16	1·670	1·189	0·714	0·250	−0·893	−1·99		
−0·25	7·65	7·48	7·30	7·14	6·97	6·64	6·33	6·03	5·73	5·18	4·61	4·07	3·56	3·06	2·57	2·09	1·607	1·132	0·660	0·197	−0·250	−1·382			
−0·3	6·94	6·78	6·61	6·45	6·29	5·97	5·66	5·36	5·07	4·52	4·00	3·49	2·99	2·50	2·016	1·540	1·066	0·596	0·1330	−0·318	−0·728	−1·870			
−0·35	6·26	6·11	5·94	5·78	5·62	5·31	5·01	4·73	4·45	3·92	3·41	2·91	2·43	1·951	1·475	1·006	0·540	0·081	−0·382	−0·823					
−0·4	5·57	5·42	5·26	5·11	4·96	4·64	4·47	4·10	3·83	3·31	2·82	2·33	1·860	1·392	0·929	0·472	0·019	−0·433	−0·866	−1·307					
−0·45	4·95	4·81	4·66	4·51	4·36	4·08	3·80	3·55	3·28	2·78	2·29	1·823	1·360	0·895	0·440	0	−0·500	−0·954	−1·410						
−0·5	4·32	4·18	4·04	3·90	3·76	3·50	3·24	2·98	2·55	2·24	1·760	1·294	0·838	0·389	−0·051	−0·500	−0·921								
−0·55	3·71	3·58	3·44	3·31	3·19	2·93	2·68	2·43	2·19	1·716	1·254	0·800	0·351	−0·091	−0·536	−1·000									
−0·6	3·15	3·03	2·90	2·77	2·65	2·40	2·16	1·919	1·685	1·228	0·780	0·341	−0·105	−0·540											
−0·7	2·15	2·04	1·924	1·81	1·697	1·473	1·25	1·026	0·804	0·357	−0·091														
−0·8	1·29	1·181	1·074	0·967	0·859	0·644	0·429	0·215	0	−0·429															
−0·9	0·575	0·472	0·368	0·265	0·163	−0·043	−0·248																		

f. p. 372

Table 3a. $\sigma^{1/3}F_4$ vs. B and $\sigma^{1/3}(\Delta_4^2/\nu)(du_G/dx)$ for $\sigma \to \infty$ and $B \geqslant 0$

B \ $\sigma^{2/3}\left(\frac{\Delta_4^2}{\nu}\frac{du_G}{dx}\right)$	0	1	2	3	4	5	6	7	8	9	10	12·5	15	17·5	20	22·5	25	30	35	40	45	50	60	70	80	90	100
0	8·716	4·128	0·837	−1·913																							
0·5	13·95	9·03	5·18	1·95	0·920	−3·56																					
1	19·79	14·65	10·41	5·76	3·53	0·565	−2·204	−4·83																			
1·5	26·10	20·85	16·31	12·34	8·78	5·52	2·48	−0·356	−3·134																		
2	33·02	27·68	22·93	18·70	14·85	11·21	8·00	4·89	1·929	−0·911	−3·668																
2·5	40·35	34·96	30·06	25·61	21·53	17·75	14·21	10·86	7·69	4·55	1·719	−5·192															
3	48·14	42·71	37·70	33·07	28·79	24·80	21·04	17·49	14·10	10·87	7·771	−0·437															
3·5	56·37	50·89	45·8	41·99	36·53	32·42	28·54	24·66	21·17	17·73	14·45	6·711	−0·527	−7·364													
4	65·02	59·52	54·36	49·49	45·03	40·56	35·46	32·54	28·80	25·19	21·75	13·60	6·308	−1·166	−8·002												
4·5	74·07	68·56	63·28	58·34	53·64	49·18	44·93	40·87	36·98	33·23	29·62	21·07	13·14	5·634	−1·503												
5	83·52	78·02	72·69	67·69	62·37	58·28	53·90	49·89	46·01	42·24	38·61	29·12	20·81	13·02	5·57	−1·554	−8·428										
5·5	93·35	87·86	82·50	77·20	72·53	67·81	63·32	58·99	54·83	50·80	46·91	37·70	29·05	20·52	13·22	5·81	−1·321	−14·90									
6	103·57	97·92	92·67	87·53	82·55	77·78	73·17	68·72	64·46	60·33	56·32	46·76	37·84	29·39	21·28	13·73	6·334	−7·733	−21·04								
6·5	114·14	108·5	102·4	91·01	92·99	88·14	83·48	78·86	74·60	70·54	66·16	56·31	47·10	38·27	33·05	22·14	14·52	−0·0193	−13·75	−26·30							
7	125·03	119·5	114·1	108·9	104·3	98·88	94·1	89·47	85·10	80·66	76·45	66·34	56·82	47·84	39·25	31·05	22·19	8·202	−5·962	−19·45	−32·48						
7·5	136·36	130·8	125·4	120·1	115·3	110·01	105·2	100·5	95·89	91·44	87·12	76·80	67·02	57·78	48·95	40·48	32·35	16·94	2·354	−11·55	−24·86	37·80					
8	148·0	142·4	137·0	131·7	126·5	121·5	116·6	110·8	107·2	102·5	98·23	87·63	77·68	68·16	59·11	50·48	42·01	26·16	11·16	−3·115	−16·81	−30·03	−55·46				
8·5	160·0	154·4	149·0	143·6	138·4	133·25	124·8	123·6	118·9	114·2	109·74	98·97	88·76	79·00	69·70	60·75	52·17	35·83	20·47	5·790	−8·27	−21·79	−47·75	−72·59			
9	172·3	166·7	161·2	155·9	151·7	145·6	140·6	135·8	131·0	126·4	121·6	110·6	100·2	90·28	80·74	71·60	62·79	45·98	30·22	15·18	0·772	−13·12	−39·62	−64·94	−89·36		
9·5	184·5	178·9	173·5	168·2	162·7	157·7	152·6	147·7	143·0	138·2	133·5	122·4	111·7	101·6	91·85	82·51	73·48	56·27	40·09	24·73	9·96	−4·24	−31·28	−57·07	−81·91	−105·96	
10	197·9	192·3	186·8	181·6	176·0	171·0	165·9	160·5	156·1	151·1	146·6	135·7	124·4	114·2	104·1	94·55	85·31	67·71	51·08	35·36	20·25	5·70	−22·00	−48·29	−72·56	−98·05	−121·81

Table 3b. $\sigma^{2/3}F_4$ vs. B and $\sigma^{2/3}(\Delta_4^2/\nu)(du_G/dx)$ for $\sigma \to \infty$ and $B \leqslant 0$

B \ $\sigma^{2/3}(\Delta_4^2/\nu)(du_G/dx)$	−0·2	−0·1	0	0·1	0·2	0·3	0·4	0·5	0·6	0·8	1·0	1·2	1·4	1·6	1·8	2·0	2·2	2·4	2·6	2·8	3·0
0	9·905	9·296	8·716	8·163	7·634	7·128	6·644	6·180	5·737	4·905	4·128	3·403	2·714	2·061	1·439	0·837	0·256	0·307	−0·856	−1·338	−1·913
−0·05	9·418	8·806	8·226	7·673	7·146	6·644	6·164	5·706	5·269	4·450	3·687	2·975	2·300	1·652	1·051	0·461	−0·1085	−0·662	−1·158	−1·724	
−0·1	8·938	8·323	7·742	7·190	6·666	6·167	5·691	5·240	4·810	4·004	3·257	2·558	1·900	1·274	0·674	0·0970	−0·461	−1·002	−1·567		
−0·15	8·466	7·847	7·265	6·714	6·192	5·697	5·227	4·782	4·360	3·567	2·837	2·152	1·509	0·897	0·310	−0·255	−0·802	−1·331	−1·851		
−0·2	8·001	7·378	6·795	6·245	5·726	5·235	4·772	4·334	3·919	3·142	2·427	1·758	1·132	0·532	−0·0409	−0·594	−1·128	−1·659	−2·158		
−0·25	7·544	6·916	6·331	5·782	5·266	4·781	4·324	3·894	3·487	2·727	2·024	1·377	0·765	0·180	−0·380	−0·919	−1·444	−1·954			
−0·3	7·094	6·461	5·874	5·327	4·815	4·335	3·885	3·456	3·065	2·324	1·642	1·010	0·411	−0·158	−0·705	−1·232	−1·745	−2·247			
−0·35	6·625	6·013	5·425	4·879	4·371	3·897	3·456	3·044	2·654	1·932	1·269	0·654	0·072	−0·483	−1·015	−1·532	−2·035				
−0·4	6·219	5·573	4·981	4·435	3·934	3·468	3·037	2·634	2·254	1·552	0·910	0·312	−0·254	−0·793	−1·313	−1·818					
−0·45	5·764	5·139	4·546	4·004	3·536	3·048	3·627	2·234	1·866	1·185	0·555	−0·0157	−0·294	−1·089	−1·596						
−0·5	5·378	4·713	4·117	3·577	3·086	2·638	2·228	1·847	1·491	0·834	0·233	−0·328	−0·859	−1·370							
−0·55	4·973	4·295	3·595	3·158	2·674	2·239	1·841	1·473	1·129	0·498	−0·0817	−0·623	−1·129	−1·636							
−0·6	4·578	3·885	3·230	2·747	2·273	1·850	1·466	1·113	0·781	0·1768	−0·380	−0·902									
−0·65	4·153	3·483	2·872	2·346	1·881	1·473	1·105	0·767	0·453	−0·1264	−0·650										
−0·7	3·825	3·091	2·472	1·948	1·500	1·110	0·760	0·440	0·1413	−0·410											
−0·75	3·474	2·708	2·077	1·561	1·132	0·762	0·432	0·1311	−0·1505	−0·673											
−0·8	3·146	2·335	1·689	1·183	0·775	0·431	0·1253	−0·1558	−0·419												
−0·85	2·853	1·975	1·304	0·814	0·438	0·1228	−0·1577	−0·417													
−0·9	2·613	1·635	0·919	0·456	0·1210	−0·1587	−0·352														
−0·95	2·556	1·343	0·524	0·1120	−0·1651	−0·403															

Table 4a. E_4 vs. B and $(\Delta_4^2/\nu)(\mathrm{d}u_G/\mathrm{d}x)$, and p and q vs. B for $\sigma = 0{\cdot}7$ and $B \geqslant 0$

B	p	q	$(\Delta_4^2/\nu)(\mathrm{d}u_G/\mathrm{d}x)$ 0	1	2	3	4	5	6	7	8	9	10	15	20	25	30	40	50	60	70	80	90	100	110	120	130	140
0	11·7	2·86	0	−0·76	−0·83	−0·53	−0·05	0·50																				
0·5	22·1	3·11	0	−1·8	−2·3	−2·4	−2·1	−1·6	−0·9	−0·1	0·8																	
1	34·0	3·31	0	−2·3	−3·2	−3·5	−3·4	−3·2	−2·9	−2·3	−1·7	−1·0	−0·24	4·0														
1·5	49·2	3·54	0	−2·7	−4·5	−5·5	−5·8	−5·8	−5·5	−5·0	−4·5	−4·0	−3·3	1·9														
2	65·7	3·74	0	−2·9	−4·9	−6·3	−7·2	−7·5	−7·4	−7·3	−7·1	−6·6	−6·0	−2·9	3·3													
2·5	86·5	3·94	0	−3·2	−5·6	−7·1	−8·4	−9·1	−9·6	−9·9	−10·2	−10·4	−10·3	−7·3	−2·25	4·4												
3	110·0	4·11	0	−3·5	−6·1	−8·6	−10·3	−11·8	−13·2	−14·2	−14·9	−15	−14·9	−12·4	−8·4	−2·35	5											
3·5	135	4·30	0	−4·0	−7·6	−10·4	−12·5	−14·4	−16·1	−17·5	−18·6	−19·6	−20	−18·2	−14	−8·7	−2·2	10·6										
4	164	4·47	0	−4·5	−8·7	−12·1	−15·1	−17·7	−19·6	−21·2	−22·5	−23·6	−24·4	−24	−20·5	−16	−10	−6	25·5									
4·5	195·5	4·64	0	−5·0	−9·2	−13·4	−16·7	−19·5	−22·4	−24·3	−26·4	−27·8	−29·1	−31	−28	−23	−18	−4	15	39								
5	230	4·80	0	−5·6	−10·4	−15·1	−18·8	−22·1	−25	−27·5	−29·5	−31·2	−33·0	−38	−37	−32	−27	−13	4·8	28								
5·5	266	4·95	0	−6·3	−11·4	−16·1	−20·3	−23·9	−27·2	−30·2	−33	−35·3	−37·5	−44·5	−45	−42	−37·5	−23	−6·4	15	39							
6	309	5·10	0	−7	−13·1	−18·7	−23·5	−28·1	−32·4	−36·5	−40	−43	−45·5	−54·5	−56	−54·5	−51	−39	−23	−1·5	23·5							
6·5	352	5·25	0	−7·5	−14	−20	−25·5	−31	−35·5	−39	−43	−47	−50	−60	−66	−67	−64·5	−53	−36	−15	6·5	32						
7	398	5·38	0	−8	−15	−22	−27·5	−32	−37	−41·5	−45	−49	−52·5	−65·5	−73	−71·5	−77·5	−67	−51	−33	−10	16						
7·5	446	5·50	0	−8·7	−16	−22	−29	−34	−39	−43	−48	−52	−55	−70	−81	−86	−86·5	−82	−68	−49	−27·5	−3	24	54				
8	497·5	5·62	0	−9·3	−17·5	−24	−30	−35·5	−41	−46	−51	−54	−58	−76	−89	−97	−100	−98	−86	−67·5	−47	−23	4	34				
8·5	551	5·74	0	−10	−18	−25	−32	−37	−44	−50	−55	−58	−62	−83	−99	−109	−114	−114	−99	−82	−62	−39	−14	−12	45			
9	610	5·85	0	−11	−19·5	−27	−34	−41	−49	−55	−59	−65	−70	−94	−113·5	−124·5	−131·4	−133·5	−122·5	−105·5	−86	−63·5	−38	−12·5	16·5	50		
9·5	671	5·96	0	−12	−21	−29	−37	−45	−53	−59	−68	−74·5	−81	−106	−127·8	−141	−147	−153	−143·5	−127	−109	−89	−63	−38	−15·4	23	57	
10	730	6·08	0	−13	−23	−32	−41	−50	−58	−65	−73	−80	−88	−114	−134	−149	−159	−165	−161	−148	−131	−110	−86	−61	−31	0	35	72

Table 4b. E_4 vs. B and $(\Delta_4^2/\nu)(\mathrm{d}u_G/\mathrm{d}x)$, and p and q vs. B for $\sigma = 0{\cdot}7$ and $B \leqslant 0$

B	p	q	$(\Delta_4^2/\nu)(\mathrm{d}u_G/\mathrm{d}x)$ 0	0·05	0·10	0·15	0·2	0·3	0·4	0·5	0·6	0·8	1·0	1·2	1·4	1·6	1·8	2·0	2·2	2·4	2·6	2·8	3·0	3·5	4·0	4·5	5·0
0	11·7	2·86	0	−0·076	−0·160	−0·215	−0·280	−0·395	−0·490	−0·560	−0·601	−0·693	−0·760	−0·818	−0·834	−0·849	−0·85	−0·833	−0·800	−0·753	−0·690	−0·616	−0·534	−0·300	−0·051	0·192	0·50
−0·05	10·85	2·82	0	−0·067	−0·147	−0·194	−0·250	−0·338	−0·409	−0·472	−0·526	−0·607	−0·667	−0·710	−0·733	−0·738	−0·729	−0·702	−0·659	−0·598	−0·525	−0·452	−0·376	−0·164	0·070	0·348	
−0·1	9·98	2·78	0	−0·060	−0·125	−0·173	−0·230	−0·293	−0·350	−0·400	−0·445	−0·529	−0·580	−0·622	−0·64	−0·642	−0·618	−0·577	−0·525	−0·467	−0·399	−0·326	−0·250	0·038	0·189	0·475	
−0·15	9·18	2·73	0	−0·048	−0·109	−0·152	−0·181	−0·255	−0·308	−0·355	−0·398	−0·465	−0·520	−0·554	−0·56	−0·551	−0·523	−0·485	−0·440	−0·382	−0·320	−0·241	−0·163	0·064	0·200		
−0·2	8·41	2·70	0	−0·041	−0·090	−0·129	−0·163	−0·230	−0·280	−0·320	−0·358	−0·420	−0·458	−0·482	−0·47	−0·440	−0·40	−0·360	−0·313	−0·260	−0·201	−0·136	−0·060	0·1	0·3		
−0·25	7·65	2·65	0	−0·036	−0·082	−0·115	−0·150	−0·214	−0·260	−0·300	−0·333	−0·373	−0·393	−0·296	−0·38	−0·350	−0·310	−0·263	−0·213	−0·158	−0·100	−0·033	−0·050	0·243			
−0·3	6·94	2·61	0	−0·031	−0·070	−0·102	−0·132	−0·191	−0·240	−0·273	−0·300	−0·328	−0·333	−0·321	−0·297	−0·266	−0·226	−0·180	−0·132	−0·080	−0·021	0·050	0·170	0·325			
−0·35	6·26	2·57	0	−0·023	−0·063	−0·094	−0·125	−0·179	−0·220	−0·247	−0·264	−0·285	−0·280	−0·262	−0·233	−0·197	−0·159	−0·114	−0·066	−0·011	0·040	0·112	0·185				
−0·4	5·57	2·52	0	−0·021	−0·057	−0·083	−0·110	−0·168	−0·190	−0·210	−0·227	−0·240	−0·232	−0·214	−0·182	−0·146	−0·105	−0·058	−0·007	0·045	0·116	0·179					
−0·45	4·95	2·48	0	−0·018	−0·045	−0·068	−0·090	−0·122	−0·147	−0·165	−0·178	−0·190	−0·177	−0·151	−0·120	−0·087	−0·046	0	0·0053	0·048	0·193						
−0·5	4·32	2·43	0	−0·015	−0·035	−0·053	−0·070	−0·095	−0·113	−0·127	−0·136	−0·140	−0·130	−0·110	−0·080	−0·043	−0·003	0·040	0·109								
−0·55	3·71	2·38	0	−0·011	−0·026	−0·039	−0·049	−0·067	−0·080	−0·089	−0·092	−0·090	−0·076	−0·054	−0·027	0·007	0·048	0·050									
−0·6	3·15	2·33	0	−0·008	−0·019	−0·027	−0·034	−0·050	−0·062	−0·066	−0·067	−0·058	−0·040	−0·013	0·007	0·038											
−0·7	2·15	2·24	0	−0·001	−0·002	−0·004	−0·005	−0·005	−0·0045	−0·004	−0·002	−0·001	0·0005														
−0·8	1·29	2·15	0	0	−0·001	−0·001	−0·001	−0·001	−0·001	0	0	0·001															
−0·9	0·575	2·06	0	0	−0·001	0·001	0	0	0·001																		

Table 5a. $\sigma^{2/3}E$ vs. B and $\sigma^{2/3}(\Delta_4^2/\nu)(du_G/dx)$, and $\sigma^{2/3}p$ and q vs. B for $\sigma \to \infty$ and $B \geqslant 0$

B	$\sigma^{2/3}p$	q	0	1	2	3	4	5	6	7	8	9	10	12·5	15	17·5	20	22·5	25	30	35	40	45	50	60	70	80	90
0	8·716	3·805	0	−0·783	−0·269	0·786																						
0·5	13·96	3·805	0	−1·13	−1·18	−0·60	0·335	1·50																				
1	19·79	3·805	0	−1·33	−1·77	−1·61	−1·04	−0·196	0·84	2·018																		
1·5	26·10	3·805	0	−1·45	−2·18	−2·35	−2·1	−1·56	−0·79	0·136	1·203																	
2	33·02	3·805	0	−1·53	−2·48	−2·90	−2·95	−2·68	−2·19	−1·49	−0·651	0·219	1·387															
2·5	40·35	3·805	0	−1·59	−2·69	−3·33	−3·61	−3·58	−3·32	−2·86	−2·23	−1·46	−0·586	2·016														
3	48·14	3·805	0	−1·63	−2·83	−3·66	−4·13	−4·32	−4·27	−4·02	−3·60	−3·03	−2·322	0·143														
3·5	56·37	3·805	0	−1·68	−2·96	−3·97	−4·55	−4·93	−5·00	−5·08	−4·76	−4·40	−3·87	−2·099	0·175	2·85												
4	65·02	3·805	0	−1·70	−3·05	−4·12	4·80	−5·44	−5·73	−5·85	−5·78	−5·59	−5·22	−3·86	−1·94	0·40	3·08											
4·5	74·07	3·805	0	−1·71	−3·23	−4·32	−5·21	−5·87	−6·31	−6·57	−6·65	−6·60	−6·40	−5·44	−3·86	−1·847	0·52											
5	83·52	3·805	0	−1·70	−3·22	−4·42	−5·43	−6·22	−6·79	−7·20	−7·41	−7·51	−7·46	−6·84	−5·64	−3·91	−1·85	0·54	3·18									
5·5	93·35	3·805	0	−1·69	−3·24	−4·74	−5·63	−6·52	−7·2	−7·73	−8·08	−8·31	−8·39	−8·09	−7·23	−5·84	−4·03	−1·93	0·455	5·86								
6	103·57	3·805	0	−1·85	−3·29	−4·63	−5·77	−6·77	−7·57	−8·22	−8·67	−9·00	−9·20	−9·25	−8·76	−7·59	−6·19	−4·23	−2·11	2·84	8·57							
6·5	114·14	3·805	0	−1·70	−4·1	−4·72	−5·93	−6·98	−7·83	−8·65	−9·10	−9·36	−9·93	−10·27	−9·97	−11·18	−7·99	−6·39	−4·49	0·0011	5·29	11·16						
7	125·06	3·805	0	−1·80	−3·4	−4·8	−5·1	−7·17	−8·15	−8·97	−9·54	−10·17	−10·60	−11·17	−11·18	−10·65	−9·73	−8·41	−6·76	−2·72	2·14	7·67	13·67					
7·5	136·36	3·805	0	−1·8	−3·4	−4·8	−6·1	−7·33	−8·3	−9·2	−9·97	−10·68	−11·19	−12·00	−12·27	−11·99	−11·31	−10·27	−8·88	−5·27	−0·83	4·29	10·01	16·08				
8	148·0	3·805	0	−1·8	−3·4	−4·9	−6·3	−7·5	−9·0	−10·6	−10·4	−11·2	−11·72	−12·76	−13·25	−13·25	−12·79	−11·99	−10·86	−7·69	−3·66	1·08	6·42	12·22	28·84			
8·5	160·0	3·805	0	−1·8	−3·4	−5·0	−6·4	−7·6	−8·7	−9·7	−10·6	−11·5	−12·2	−13·4	−14·16	−14·39	−14·18	−13·58	−10·68	−10	−6·33	−1·99	2·98	8·48	10·57	33·7		
9	172·3	3·805	0	−1·8	−3·4	−5·0	−6·4	−7·7	−8·9	−9·9	−10·9	−11·6	−12·6	−14·1	−15	−15·42	−15·45	−15·08	−14·37	−12·16	−8·89	−4·91	−0·292	4·84	16·39	29·12	42·75	
9·5	184·5	3·805	0	−1·8	−3·4	−4·9	−6·6	−7·8	−9·1	−10·2	−11·1	−12·1	−13·0	−14·6	−15·8	−16·4	−16·59	−16·42	−15·93	−14·12	−11·27	−7·61	−3·35	1·47	12·48	24·74	37·95	52·45
10	197·9	3·805	0	−1·8	−3·5	−4·9	−6·7	−7·9	−9·2	−10·4	−11·4	−12·6	−13·3	−14·7	−16·5	−17·2	−17·7	−17·77	−17·49	−16·07	13·67	−10·37	−6·45	−1·98	8·37	20·13	32·91	46·47

Table 5b. $\sigma^{2/3}E$ vs. B and $\sigma^{2/3}(\Delta_4^2/\nu)(du_G/dx)$, and $\sigma^{2/3}p$ and q vs. B for $\sigma \to \infty$ and $B \leqslant 0$

B	$\sigma^{2/3}p$	q	−0·2	−0·1	0	0·1	0·2	0·3	0·4	0·5	0·6	0·8	1·0	1·2	1·4	1·6	1·8	2·0	2·2	2·4	2·6	2·8	3·0
0	8·716	3·805	0·428	0·199	0	−0·173	−0·321	−0·447	−0·550	−0·634	−0·696	−0·967	−0·783	−0·747	−0·675	−0·561	−0·428	−0·269	−0·089	0·109	0·321	0·550	0·786
−0·05	8·226	3·805	0·431	0·200	0	−0·172	−0·319	−0·440	−0·540	−0·617	−0·674	−0·732	−0·734	−0·685	−0·599	−0·476	−0·326	−0·155	−0·368	0·244	0·470	0·704	
−0·1	7·742	3·805	0·435	0·201	0	−0·171	−0·315	−0·433	−0·529	−0·599	−0·649	−0·695	−0·680	−0·618	−0·517	−0·380	−0·219	−0·0348	0·167	0·388	0·684		
−0·15	7·265	3·805	0·440	0·202	0	−0·170	−0·312	−0·425	−0·516	−0·580	−0·622	−0·654	−0·623	−0·547	−0·429	−0·280	−0·106	0·090	0·304	0·536	0·777		
−0·2	6·785	3·805	0·445	0·203	0	−0·169	−0·308	−0·418	−0·501	−0·558	−0·593	−0·609	−0·563	−0·471	−0·336	−0·175	0·0133	0·221	0·448	0·687	0·940		
−0·25	6·331	3·805	0·452	0·205	0	−0·168	−0·304	−0·408	−0·485	−0·534	−0·561	−0·560	−0·498	−0·388	−0·239	−0·063	0·138	0·360	0·596	0·847	1·107		
−0·3	5·874	3·805	0·459	0·206	0	−0·167	−0·298	−0·398	−0·467	−0·508	−0·526	−0·506	−0·427	−0·298	−0·136	0·056	0·270	0·504	0·752	1·011	1·281		
−0·35	5·425	3·805	0·466	0·208	0	−0·165	−0·293	−0·386	−0·447	−0·478	−0·488	−0·449	−0·351	−0·205	−0·0257	0·181	0·410	0·654	0·912	1·182			
−0·4	4·981	3·805	0·477	0·210	0	−0·164	−0·286	−0·372	−0·422	−0·445	−0·444	−0·385	−0·266	−0·103	0·092	0·314	0·055	0·811	1·080				
−0·45	4·546	3·805	0·487	0·213	0	−0·161	−0·279	−0·356	−0·397	−0·409	−0·397	−0·317	−0·176	0·0047	0·217	0·453	0·767	0·975					
−0·5	4·117	3·805	0·500	0·216	0	−0·159	−0·270	−0·337	−0·367	−0·367	−0·343	−0·239	−0·079	0·122	0·352	0·602	0·868						
−0·55	3·695	3·805	0·516	0·220	0	−0·156	−0·260	−0·314	−0·332	0·319	−0·283	−0·153	0·028	0·248	0·494	0·757							
−0·6	3·280	3·805	0·537	0·224	0	−0·153	−0·246	−0·289	−0·292	−0·265	−0·214	−0·059	0·145	0·384	0·645								
−0·65	2·872	3·805	0·562	0·230	0	−0·148	−0·233	−0·258	−0·245	−0·203	−0·136	0·046	0·273	0·530									
−0·7	2·472	3·805	0·592	0·239	0	−0·143	−0·211	−0·220	−0·190	−0·129	−0·048	0·163	0·412	0·688									
−0·75	2·077	3·805	0·636	0·250	0	−0·136	−0·184	−0·174	−0·123	−0·0436	0·055	0·294	0·566										
−0·8	1·689	3·805	0·696	0·266	0	−0·125	−0·152	−0·116	−0·027	0·058	0·176	0·444											
−0·85	1·304	3·805	0·788	0·291	0	−0·109	−0·105	−0·039	−0·060	0·182	0·316	0·616											
−0·9	0·919	3·805	0·933	0·335	0	−0·083	−0·037	0·063	0·251														
−0·95	0·524	3·805	1·311	0·438	0	−0·0316	0·072																

Table 6. Comparison of $\sigma^{2/3}F_4$ and $\sigma^{2/3}(\Delta_4^2/\nu)(du_G/dx)$ from Table 2 ($\sigma = 0{\cdot}7$) and Table 3 ($\sigma = \infty$) for $\beta = 0$ and $\beta = 1$ and several B values

	$\sigma^{2/3}F_4$		$\sigma^{2/3}(\Delta_4^2/\nu)(du_G/dx)$	
β	0		1	
B \ σ	0·7 (Table 2)	∞ (Table 3)	0·7 (Table 2)	∞ (Table 3)
−0·8	1·010	1·689	0·879	0·444
−0·6	2·48	3·28	1·170	0·862
−0·4	4·40	4·98	1·748	1·309
−0·2	6·64	6·80	2·48	1·786
0	9·23	8·72	3·24	2·29
1	26·8	19·79	8·10	5·20
2	51·9	33·0	13·90	8·68
3	86·8	48·1	21·1	12·65
4	129·3	65·0	29·0	17·09
5	181·2	83·5	37·8	21·9
6	244	103·6	47·9	27·2
7	314	125·1	58·4	32·9
8	392	148·0	69·9	38·9
9	481	172·4	82·0	45·3
10	575	197·9	94·7	48·5

Step (ii) Define non-dimensional quantities as follows:

$$u_G^{**} \equiv u_G/U \tag{25}$$

$$x^{**} \equiv (1/L)\int_0^x (R/R_0)^2\,dx \tag{26}$$

$$\Delta_4^{**} \equiv \Delta_4\,(R/R_0)\,\sqrt{(U/L\nu)} \tag{27}$$

where R is the distance of the surface element from the axis of symmetry.

The differential equation to be solved thus becomes:—

$$u_G^{**}\frac{d\Delta_4^{**2}}{dx^{**}} = F_4\left(\Delta_4^{**2}\frac{du_G^{**}}{dx^{**}}, B, \sigma\right). \tag{28}$$

Step (iii) From the data of the problem, and from (25) and (26), tabulate values of u_G^{**} and du_G^{**}/dx^{**} for various values of x^{**}

Step (iv) Solve (28) by standard procedures, referring to the appropriate table for values of F_4. [Note that $\Delta_4^{**2}(du_G^{**}/dx^{**})$ is identical in value with $(\Delta_4^2/\nu)(du_G/dx)$, by reason of the definitions.]

3.4. *Starting conditions*

The solution of a first-order differential equation requires the specification of a boundary condition. This is usually given, in boundary-layer problems, at the upstream extremity of the boundary layer where it is usual to take x (or x^*, or x^{**}) as zero. The three important cases arising in practice will now be discussed.

Body with a sharp leading edge. If the leading edge of the surface engaging in mass transfer is sharp, the boundary-layer thickness is zero there. The starting condition for the numerical integration is thus:

$$x = 0, \qquad \Delta_4 = 0. \tag{29}$$

Although this condition is quite adequate from the mathematical point of view, provided that u_G is not simultaneously zero, it should be remembered that the conclusion that $\Delta_4 = 0$, is unrealistic in practice for two distinct reasons. The first reason is that no practical edge can be sharp, in the sense of having zero radius of curvature; the second is that the boundary layer equations themselves cease to be valid in the vicinity of an edge. These facts are well known and require no detailed comment here.

Stagnation point of a two-dimensional body. The second important case is that of the two-dimensional surface which does *not* possess a sharp leading edge. Such a surface exhibits a stagnation point, in the neighbourhood of which the velocity outside the boundary layer increases linearly with x, the zero of the latter dimension corresponding with the stagnation point. Thus we have:

$$u_G = \left(\frac{du_G}{dx}\right)_0 x \tag{30}$$

suffix 0 here indicating the vicinity of $x = 0$.

The difficulty presented by this case is that the starting condition does not immediately yield an initial value of Δ_4^* with which to begin the integration. The way out of the difficulty lies through the recognition that (23) ensures that F_4 equals zero where u_G^* equals zero,† i.e. at $x^* = 0$. Now, since B and σ are known, the value of $\Delta_4^{*2}(du_G^*/dx^*)$ for which $F_4 = 0$ can be learned by inspection of the tables of the auxiliary function, F_4. The starting value of the boundary-layer thickness is then deduced from:

$$\Delta_4^{*2} = \left[\Delta_4^{*2}\frac{du_G^*}{dx^*}\right]\Big/\left(\frac{du_G^*}{dx^*}\right). \tag{31}$$

Equation (31) is easily evaluated since $(du_G^*/dx^*)_0$ is given in the data of the problem. It is equal to $(L/U)(du_G/dx)_0$. Clearly Δ_4^{*2} is independent of x^* near the stagnation point.

Stagnation point of an axi-symmetrical body. Near the stagnation point of an axi-symmetrical body, the velocity distribution is given once more by the equation:

$$u_G = \left(\frac{du_G}{dx}\right)_0 x. \tag{32}$$

This starting condition fails to show immediately what is the initial value of Δ_4^{**}, and therefore must be re-arranged before the numerical integration of equation (28) can begin. This re-arrangement now follows; the useful result will be found in the last two paragraphs of the present section.

A characteristic of the stagnation-point region is that x and R are identical there.

† Unless $d\Delta_4^{*2}/dx^*$ is infinite, which is physically implausible.

Inserting this fact in the definition (26) and integrating, we deduce the relation between x^{**} and x; it is:

$$x^{**} = \frac{1}{3}\frac{x^3}{LR_0^2}. \tag{33}$$

Replacing u_G and x in (32) by $u_G{}^{**}$ and x^{**}, we then deduce:

$$u_G{}^{**} = \frac{(3LR_0^2)^{1/3}}{U}\left(\frac{du_G}{dx}\right)_0 x^{**1/3}. \tag{34}$$

This exponential relation between $u_G{}^{**}$ and x^{**} ensures that locally the boundary layer is described by one of the exact "similar" solutions of the boundary-layer equations. Which solution is relevant is discovered in the following way. Since the boundary layer is "similar", the two quantities $(\Delta_4{}^{**2}\, du_G{}^{**}/dx^{**})$ and $(u_G{}^{**}\, d\Delta_4{}^{**2}/dx^{**})$ (i.e. F_4) have fixed values. What are these values? Evidently, by reason of (34):

$$\Delta_4{}^{**2}\frac{du_G{}^{**}}{dx^{**}} = \Delta_4{}^{**2}\frac{(3LR_0^2)^{1/3}}{3U}\left(\frac{du_G}{dx}\right)_0 x^{**\,-2/3} \tag{35}$$

which can be re-written as:

$$\Delta_4{}^{**2} = \frac{\left(\Delta_4{}^{**2}\dfrac{du_G{}^{**}}{dx^{**}}\right)}{\dfrac{(3LR_0^2)^{1/3}}{3U}\left(\dfrac{du_G}{dx}\right)_0} x^{**2/3}. \tag{36}$$

Differentiating (36) we deduce:

$$\frac{d\Delta_4{}^{**2}}{dx^{**}} = \frac{2\left(\Delta_4{}^{**2}\dfrac{du_G{}^{**}}{dx^{**}}\right)}{\dfrac{(3LR_0^2)^{1/3}}{U}\left(\dfrac{du_G}{dx}\right)_0} x^{**\,-1/3} \tag{37}$$

which can be re-written, by reason of (34) as:

$$u_G{}^{**}\frac{d\Delta_4{}^{**2}}{dx^{**}} = 2\left(\Delta_4{}^{**2}\frac{du_G{}^{**}}{dx^{**}}\right). \tag{38}$$

Equation (38) is the relation which enables us to find the starting condition for the numerical integration; for it tells us that we must find that value of F_4, for the prescribed values of B and σ, which is twice the corresponding value of $\Delta_4{}^{**2}\, du_G{}^{**}/dx^{**}$. Such values lie on lines of slope 2 in Figs. 5 and 6; reference to these, or corresponding tables, is the best way of determining the required quantities.

Once the value of $\Delta_4{}^{**2}\, du_G{}^{**}/dx^{**}$ has been found in this way, values of $\Delta_4{}^{**2}$ can be evaluated in the vicinity of $x^{**} = 0$ from equation (36). Numerical integration of (28) can now proceed without difficulty.

3.5. *Quadrature procedure*

The parallels between the procedure recommended in the present section and that for the velocity boundary layer in Paper 1 are so close and numerous as to make comment unnecessary. Certainly it will be no surprise to find that quadrature procedures for solving equations (17), (23) and (28) are as helpful here as they were found to be in Paper 1. The use of the quadrature procedure is the main point in which the method of Smith and Spalding [5, 19] differs from that of Eckert [6, 15]. We shall first describe the quadrature method, and provide tables of the relevant quantities. Finally the method will be still further simplified in the interests of speedy computation.

Linear approximations to the F_4 functions. The quadrature procedure derives from the recognition that the curves appearing in Figs. 5 and 6 can be approximately represented by straight lines. Indeed, without approximation, we can write:

$$F_4 = p - \frac{q\Delta_4^2}{\nu}\frac{du_G}{dx} + E_4 \tag{39}$$

wherein p and q are functions of B and σ alone, while E_4 is a function of B, σ and

$$(\Delta_4^2/\nu)\,(du_G/dx).$$

The point of the substitution (39) becomes apparent if we choose p and q so that E_4 is small. This may be done by making p equal to the value of F_4 when $(\Delta_4^2/\nu)\,(du_G/dx)$ is zero, and making q equal to p divided by the value of $(\Delta_4^2/\nu)(du_G/dx)$ where F_4 is zero. The significance of these substitutions is shown by Fig. 7. The curve is a

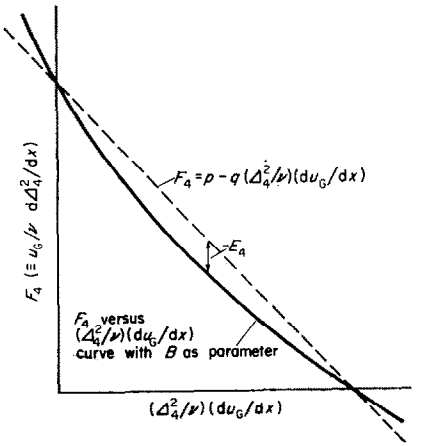

FIG. 7. Sketch illustrating the significance of p, q and E_4.

representative member of those appearing in Figs. 5 and 6, valid for a particular B and σ; the broken straight line is the linear approximation to the curve, and the vertical distance between the line and the curve is a measure of $-E_4$.

Values of p and q and E_4 corresponding to the curves appearing in Figs. 5 and 6 are given in Tables 4 and 5. In the case of Table 5, p and E_4 are of course multiplied by $\sigma^{2/3}$.

Solution as a quadrature. Equation (17) can now be combined with (39) to give, for two-dimensional boundary layers:

$$\frac{u_G}{\nu}\frac{d\Delta_4^2}{dx} = p - q\frac{\Delta_4^2}{\nu}\frac{du_G}{dx} + E_4. \qquad (40)$$

This equation may be integrated formally to give:

$$\Delta_4 = \left(\frac{\int_0^x \nu p u_G^{q-1}\,dx}{u_G^q} + \frac{\int_0^x \nu E_4 u_G^{q-1}\,dx}{u_G^q}\right)^{1/2}. \qquad (41)$$

Now since p and q have been chosen so as to make E_4 small, a first approximation to Δ_4 namely $\Delta_{4,I}$, is given by ignoring the second term in the bracket. We obtain:

$$\boxed{\Delta_{4,I} = \left(\frac{p\nu\int_0^x u_G^{q-1}\,dx}{u_G^q}\right)^{1/2}}. \qquad (42)$$

Since p and q are known, for given B and σ, while u_G is a known function of x, the right-hand side of (42) is easily evaluated.

Although equation (42) will often give sufficient accuracy to warrant accepting $\Delta_{4,I}$ as the required value of Δ_4, a second and better approximation, namely $\Delta_{4,II}$, may be obtained by the following procedure:

(i) From (42) and given values of du_G/dx evaluate $\Delta_{4,I}^2\,du_G/dx$ at each x-station considered in the quadrature.

(ii) Hence from Tables 4 and 5, evaluate $E_{4,I}$, the corresponding value of E_4 for each x-station.

(iii) Thereafter calculate $\Delta_{4,II}$ from the following expression deriving from equation (41):

$$\Delta_{4,II} = \left(\Delta_{4,I}^2 + \frac{\nu\int_0^x E_{4,I}\,u_G^{q-1}\,dx}{u_G^q}\right)^{1/2}. \qquad (43)$$

If desired, third and fourth approximations may be evaluated in a similar manner. Convergence is bound to be rapid since p and q have been chosen so as to render E_4 small.

A general formula

Quadrature formulae corresponding to equations (41), (42) and (43) can of course be written in terms of the singly-starred and doubly-starred quantities of Sections 3.2 and 3.3. The latter transformation is however only desirable as an interim measure, indicating how the radius variation R/R_0 has to be introduced into the quadrature in terms of the singly-starred quantities. We may therefore adopt the following equation as the generally valid quadrature formula:

$$\boxed{\Delta_4^* = \left[\frac{p\int_0^{x^*}(R/R_0)^2\,u_G^{*q-1}\,dx^*}{(R/R_0)^2\,u_G^{*q}} + \frac{\int_0^{x^*}(R/R_0)^2\,E_4\,u_G^{*q-1}\,dx^*}{(R/R_0)^2\,u_G^{*q}}\right]^{1/2}}. \qquad (44)$$

Two-dimensional flows can be treated by this formula by regarding them as limiting cases of axi-symmetrical ones, in which R/R_0 has a uniform value at all x^*; thus the R/R_0 terms vanish. The quantity E_4 appearing in (44) is of course the same function of $\Delta_4^{*2}\,du_G^*/dx^*$ as it is of $(\Delta_4^2/\nu)\,(du_G/dx)$.

The corresponding formula for the first approximation to Δ_4^* is obviously:

$$\Delta_{4,I}^* = \left[\frac{p\int_0^{x^*}(R/R_0)^2\,u_G^{*q-1}\,dx^*}{(R/R_0)^2\,u_G^{*q}}\right]^{1/2}. \qquad (45)$$

Further values of p and q

It would be impracticable to present tables such as Table 4 for all values of σ. However, if the first approximation to the Δ_4 distribution is regarded as sufficiently accurate, the only auxiliary functions needed are $p\ (B, \sigma)$ and $q\ (B, \sigma)$. These are provided in Fig. 8, which has been derived from the similar solutions contained in Paper 3; actually $p\,\sigma^{2/3}$ is plotted instead of p for obvious reasons.

Fig. 8, together with the quadrature formula (42) or (45), provide a convenient and simple means of predicting mass-transfer rates, often

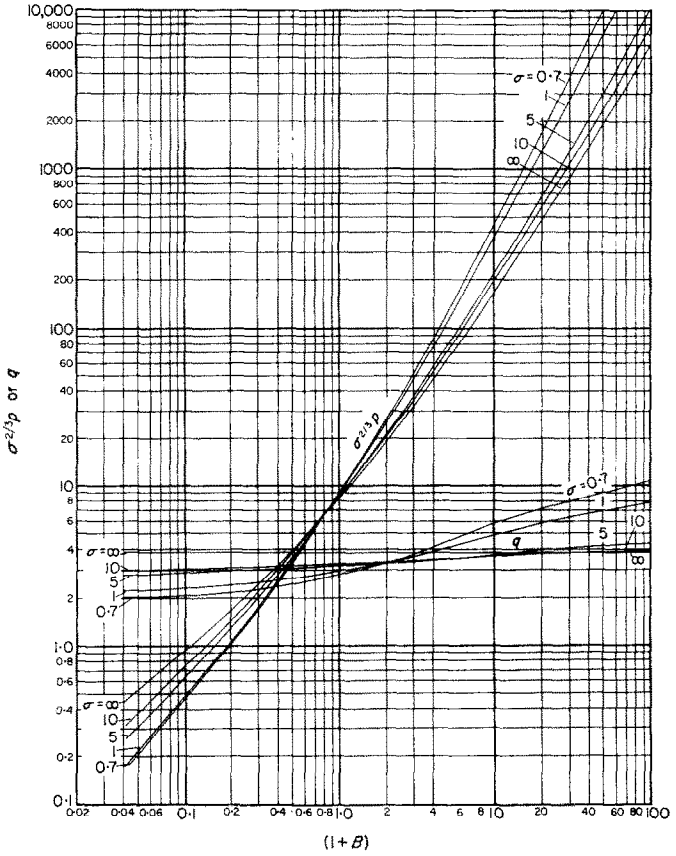

FIG. 8. $\sigma^{2/3}p$ and q vs. $(1 + B)$ for various values of σ.

with acceptable accuracy, over a wide variety of conditions.

4. APPLICATIONS OF THE METHODS OF CALCULATIONS

4.1. *Introduction*

The remainder of the paper will be devoted to the presentation and discussion of particular applications of the methods of mass-transfer predictions. The examples are chosen because of their practical importance, to illuminate a particular aspect of the theory, or to provide comparisons with the predictions of other authors.

4.2. *The axi-symmetrical stagnation point*

Practical relevance. Mass transfer occurs through the laminar boundary layers which form at axi-symmetrical stagnation points in a number of practical circumstances, for example: at the front of a sphere of burning liquid fuel suspended in an air stream [20]; on the nose of a transpiration cooled space vehicle re-entering the earth's atmosphere [21]; and on a pellet of ammonium perchlorate exposed to a perpendicular stream of hydrocarbon gas [22]. Although the fluid density and transport properties are actually non-uniform in all these cases, it is still valuable to have solutions to the differential equations of boundary layer for uniform properties; for, as has been shown [23], the variable-property solutions differ little from the uniform-property ones, in important respects, when appropriately plotted.

The axi-symmetrical stagnation point is of course a situation which gives rise to a "similar" boundary layer; this means that the methods of

the present paper are not needed for the prediction of the boundary layer-parameters, values for which can be deduced directly from Paper 3. Nevertheless, the methods given in Section 3 *may* be used; comparison of the results with exact ones gives an indication of the accuracy of the methods.

Exact solutions. Figs. 9 and 10 contain plots of $\sigma^{2/3}\, g/(\mu\rho\ \mathrm{d}u_G/\mathrm{d}x)^{1/2}$ and $\dot{m}''/(\mu\rho\ \mathrm{d}u_G/\mathrm{d}x)^{1/2}$ respectively. The abscissa is B and the parameter is σ. The curves have been constructed from the exact values presented in Paper 3, filled out by the use of the I (J, K) Tables there presented; they can be taken as accurate within ± 2 per cent.

Fig. 9 is qualitatively similar to one presented for the two-dimensional stagnation point in

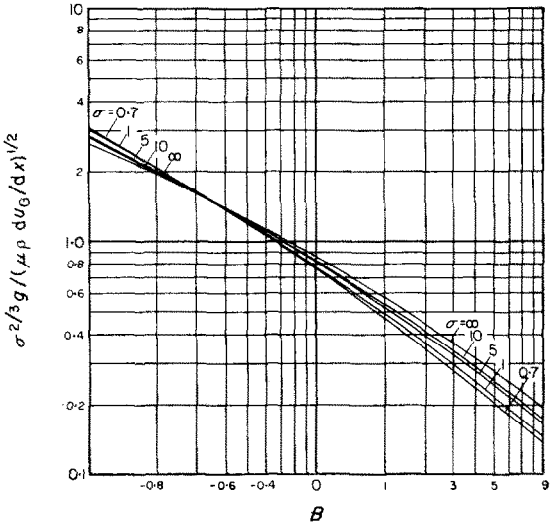

FIG. 9. Values of dimensionless mass-transfer conductance for the axi-symmetrical stagnation point ($\beta = \frac{1}{2}$) obtained as indicated in text.

Paper 3 (Fig. 6 of that paper); as usual, the conductance decreases as the driving force increases. Fig. 10 shows the influences of B and σ on the mass-transfer rate more directly.

Solutions obtained by the first approximation of Section 3.5. It has been explained already in Section 3.4 that, at the axi-symmetrical stagnation point, u_G is proportional to x [equation (30)] and x is equal to R. In these circumstances equation (45) yields:

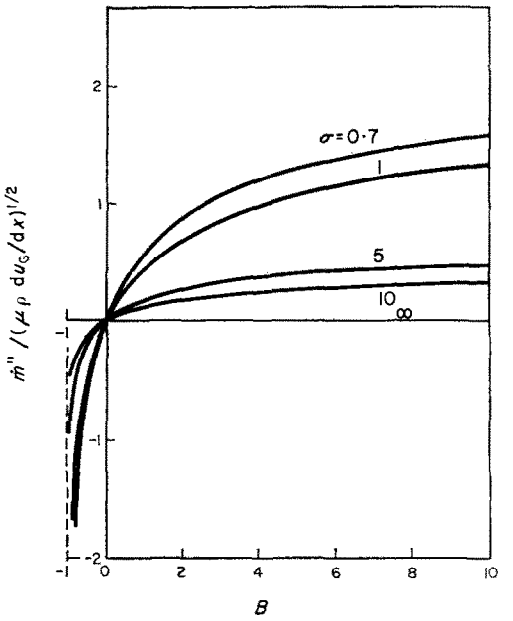

FIG. 10. Values of the dimensionless mass-transfer rate at the axi-symmetrical stagnation point ($\beta = \frac{1}{2}$) derived from Fig. 9.

$$\Delta_{4.1}^{*} = \left[\frac{p}{(q+2)\,(\mathrm{d}u_G^{*}/\mathrm{d}x^{*})}\right]^{1/2}. \qquad (46)$$

Returning to physically significant quantities by way of (24), (20) and (21), we obtain:

$$\left(\frac{\dot{m}''}{B}\right)_{\mathrm{I}} = g_{\mathrm{I}} = (1/\sigma)\,[(q+2)\,\mu\rho\,(\mathrm{d}u_G/\mathrm{d}x)/p]^{1/2} \qquad (47)$$

wherein the subscript I serves as a reminder that the first approximation is in question.

Fig. 11 contains a plot of $\sigma^{2/3}\, g_{\mathrm{I}}/[\mu\rho\ \mathrm{d}u_G/\mathrm{d}x]^{1/2}$ against B for various σ, obtained by evaluating (47) with the aid of the p and q values contained in Fig. 8. Comparison with Fig. 9 shows good qualitative agreement, and a quantitative agreement within 5 per cent over most of the range. The disagreement between the first approximation and the exact values becomes greatest when B is large and σ is small.

Solutions obtained by iteration. When the error term E_4 is introduced into the Δ_4 expression, as indicated by equation (44), (46) must be replaced by:

$$\Delta_{4}^{*} = \left[\frac{p+E_4}{(q+2)\,(\mathrm{d}u_G^{*}/\mathrm{d}x^{*})}\right]^{1/2} \qquad (48)$$

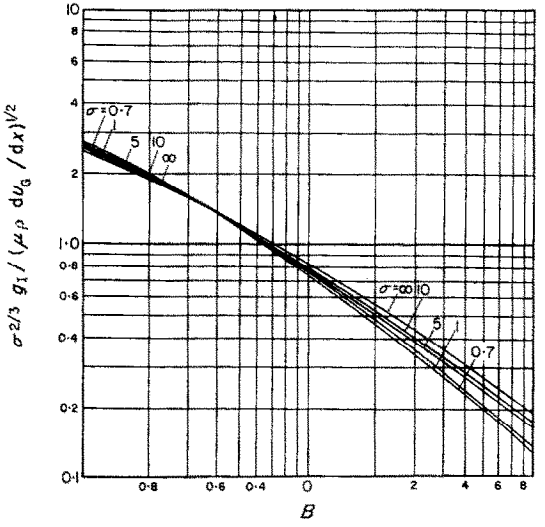

FIG. 11. Values of dimensionless mass-transfer conductance for the axi-symmetrical stagnation point ($\beta = \frac{1}{2}$), obtained by the first approximation of Section 3.5.

where E_4 depends on $(\Delta_4^2/\nu)\, du_G/dx$, B and on σ, as is shown by Table 4a, for example.

As an illustration of the use of the latter table, we determine the value of Δ_4^* for $\sigma = 0{\cdot}7$ and $B = 1$; for this case, $p = 34{\cdot}0$ and $q = 3{\cdot}37$.

The first approximation, with E_4 set equal to zero in (48), yields

$$\Delta_{4,\mathrm{I}}^{*2} \frac{du_G^*}{dx^*} = \frac{34}{3{\cdot}37 + 2} = 6{\cdot}34. \qquad (49)$$

Interpolation in Table 4a thus yields a value of $E_{4,\mathrm{I}}$ equal to $-2{\cdot}6$. Insertion of this quantity into (48) leads to the second approximation for Δ_4^* in the form:

$$\Delta_{4,\mathrm{II}}^{*2} \frac{du_G^*}{dx^*} = \frac{34 - 2{\cdot}6}{3{\cdot}37 + 2} = 5{\cdot}85. \qquad (50)$$

The resulting second approximation is correspondingly found from Table 4a, to be $-2{\cdot}8$. Substitution of this value in (48) yields the third approximation for Δ_4^* in the form:

$$\Delta_{4,\mathrm{III}}^{*2} \frac{du_G^*}{dx^*} = \frac{34 - 2{\cdot}8}{3{\cdot}37 + 2} = 5{\cdot}81. \qquad (51)$$

We may conclude that convergence is rapid; the first approximation for Δ_4^* is only about 4 per cent too large while the second is already within $\frac{1}{2}$ per cent of the asymptotic value.

Of course the asymptotic values are identical with those of Figs. 9 and 10, since Table 5 has been derived from the same family of exact solutions as have Figs. 9 and 10. There is therefore no point in making further comparisons.

Concerning the validity of the Chilton–Colburn analogy. In analyses of melting ablation at the axi-symmetrical stagnation point, Adams and Bethe [24], and Lees [25], have assumed that the shear stress at the interface is related to the mass-transfer conductance as follows:

$$\frac{\gamma s g_0}{u_G g \sigma^{2/3}} = 1. \qquad (52)$$

This relation represents a modification of the Reynolds analogy introduced by Chilton and Colburn [26].

The data in Fig. 9, together with those collected in Paper 1 and 2, enable us to test this assumption comprehensively. The result of the test is shown in Fig. 12. Evidently the Chilton–Colburn analogy under estimates the ratio of shear stress to mass-transfer conductance; it expresses the effect of σ only at large σ.

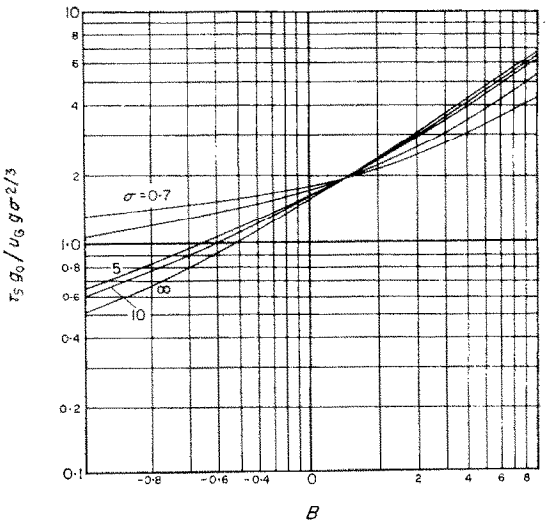

FIG. 12. A test of the Chilton–Colburn analogy for the axi-symmetrical stagnation point. Curves would collapse into a horizontal with unity ordinate if analogy were correct.

Fig. 13 contains, for interest, a corresponding test of the Chilton–Colburn analogy for the two-dimensional stagnation point. Similar conclusions may be drawn.

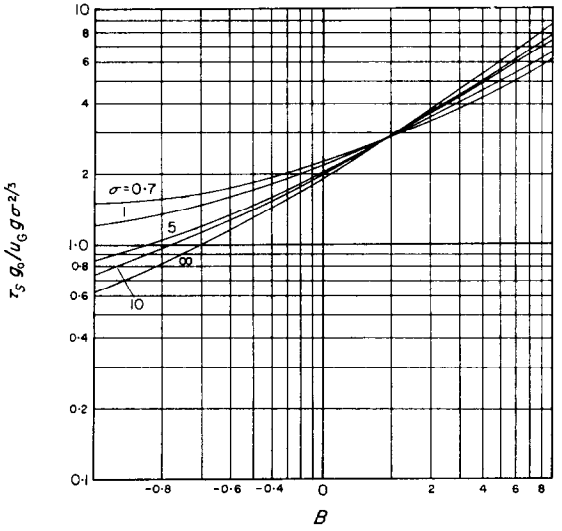

FIG. 13. A test of the Chilton–Colburn analogy for the plane stagnation point.

4.3. *The transpiration cooling of a cylinder*

We return now to the problem discussed in Section 2.3; instead of the extended Seban–Drake method, however, we here use the methods described in Section 3.5.

The results are shown in Fig. 14 wherein $(\dot{m}''l/\mu)\ (Ul/\nu)^{1/2}$ and $(\Delta_4/l)\ (Ul/\nu)^{1/2}$ are plotted against x/l. The broken curves are those obtained by the use of equation (42); the full curves result from the evaluation of (41) by successive approximations and so may be regarded as satisfying equation (17) exactly. Clearly the first approximation differs only slightly from the exact solution.

The mass-transfer rate deduced from the method of Section 3 is compared in Fig. 15 with that deduced earlier. Here it is evident that the two results are in agreement at the stagnation point but differ appreciably elsewhere. The agreement is to be expected, since the flow near the stagnation point is a "similar" one; as to the disagreement, there is no present way of telling which curve is more "correct", although it may be regarded as relevant that the Section 3

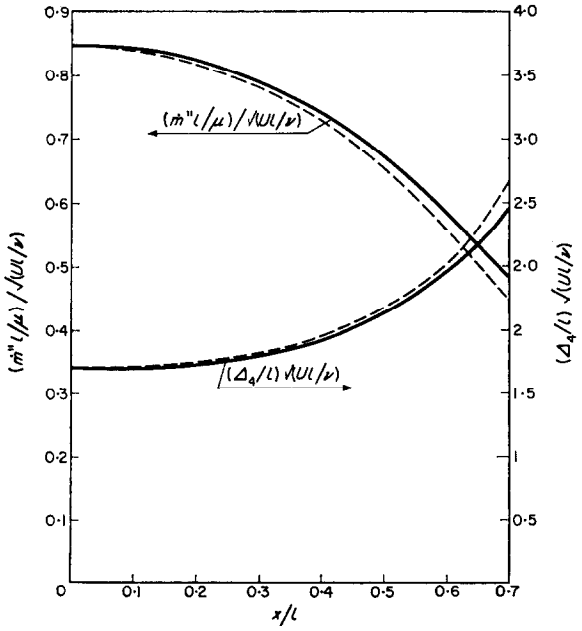

FIG. 14. Solution for transpiration cooling of a cylinder (by the method of Section 3). Dotted lines: 1st approximation; solid lines: exact solution of equation (17).

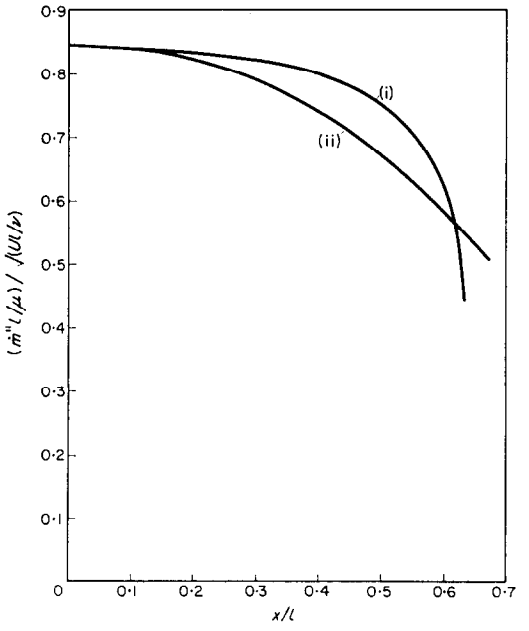

FIG. 15. Comparison of solutions for the transpiration cooling of a cylinder with $B = 1$ and $\sigma = 0{\cdot}7$. (i) By the method of Section 2. (ii) By the method of Section 3.

method agrees better than the Section 2 method with experimental data on *heat transfer* from cylinders in the absence of mass transfer [14].

4.4. *The sphere*

The application of the theory to axi-symmetrical bodies has been discussed in Section 3.4. The problems of burning of fuel droplets, transpiration cooling of nose cones, etc. are examples of this application. To illustrate it, we consider the burning of fuel droplets at Reynolds numbers which are high enough for a boundary layer to form over the front half of the sphere. The mainstream velocity distribution over the front portion of a sphere under these conditions [27] is shown in Fig. 16; this has been used, in

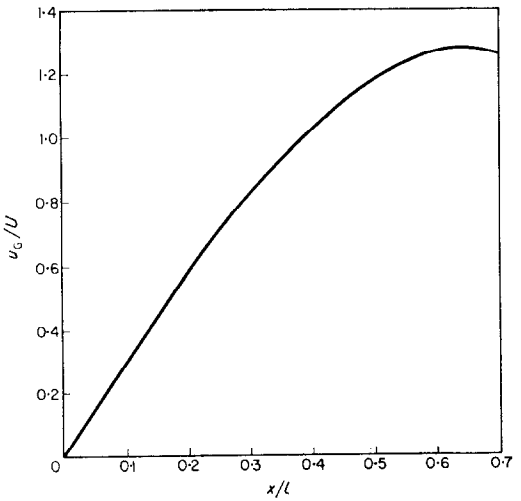

FIG. 16. Velocity distribution over the front portion of a sphere [27].

conjunction with the method of Section 3.5, to permit the calculation of the mass-transfer rate. The results for various B are shown in Fig. 17 in the form of a plot of $(\dot{m}''l/\mu)/\sqrt{(Ul/\nu)}$ against x/l wherein dotted lines are first approximations and solid lines second approximations. The latter are sufficiently exact (Section 4.2).

Experimental data are available for the *average* burning rate, $\bar{m}''$, for the whole surface of a sphere of burning liquid fuel [20]; a smooth curve through these data is shown by the broken line in Fig. 18. The transport-properties μ and ρ have been inserted at their *free*-stream values in evaluating the dimensionless value

$$\bar{m}''/\sqrt{(\mu\rho U/l)}.$$

The prediction of Fig. 17 can be compared with the experimental data only if an assumption

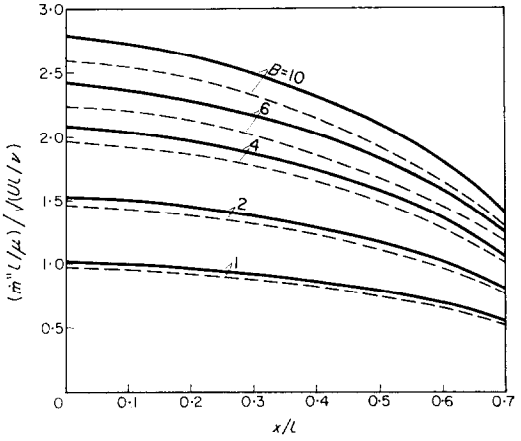

FIG. 17. Dimensionless mass-transfer distribution over the front portion of a sphere.
– – – – 1st approximation,
———2nd approximation.

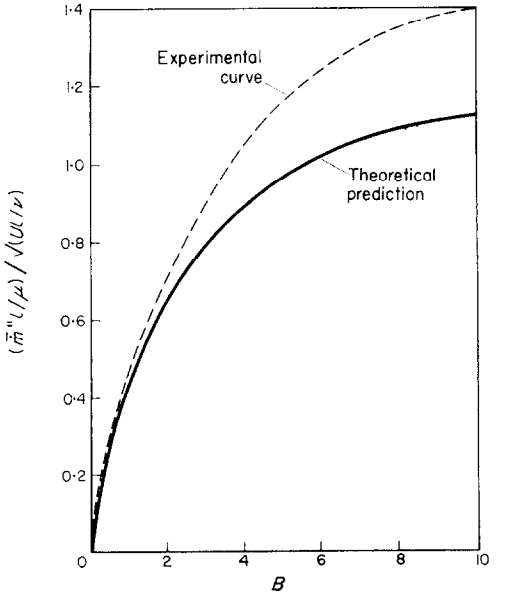

FIG. 18. Average dimensionless mass-transfer rate for a sphere. The theoretical prediction neglects the contribution of the rear half of the surface.

is made concerning the contributions of the rear half of the sphere to the total burning rate. Since it is known that this contribution is much less than that of the front half at this Reynolds number, we shall assume that it is zero. Then a theoretical value of $\bar{m}''/\sqrt{(\mu\rho U/l)}$ can be obtained from Fig. 17 by evaluation of the quadrature:

$$\bar{m}''\pi l^2 = \int_0^{l/2} \dot{m}'' \,.\, 2\pi R \,\mathrm{d}x. \qquad (53)$$

The corresponding curve is marked as a full line in Fig. 18.

It is seen that the experimental and theoretical curves lie close together. The latter lies somewhat below the former as is to be expected; for the complete neglect of mass transfer from the rear half of the sphere is certainly too extreme an assumption.

4.5. *The flat plate*

As a final example of the application of the present methods, we consider the burning of steel from a flat surface along which flows a stream of oxygen; it will be supposed that the boundary layer is laminar. This example is chosen more so as to emphasize the practical applicability of the theory as a whole than to illustrate the mathematical techniques which form the focus of attention in the present paper; for the boundary layer on a flat plate is of course a "similar" one.

Nature of process. In the process of burning of steel, oxygen diffuses to the surface of steel and reacts with it to form iron oxide and carbon monoxide. Being non-volatile, the iron oxide pours away from the surface of the steel as liquid slag. Consequently, the net substance transferred to the combustion face of steel is the amount of oxygen diffused to the surface minus the amount of carbon monoxide formed. Moreover, the reaction between oxygen and steel is exothermic, and most of the heat of reaction is used in melting the steel. This molten metal also pours away from the surface. The total rate of disappearance of steel from the surface is, therefore, the sum of the burning rate and the melting rate; it can be calculated from, a knowledge of the gas transferred to the surface of steel, the reaction heat balance and the composition of the steel.

Driving force. For steel comprising iron and carbon, the driving force can be written [28] as:

$$B = -\frac{(1 - n_c)r_i - n_c}{(1 - n_c)r_i - n_c r_c} m_{O,G} \qquad (54)$$

where B = driving force,
n_c = mass of carbon per unit mass of steel,
r_c = mass of oxygen which combines with unit mass of carbon to form CO,
r_i = mass of oxygen which combines with unit mass of iron to form Fe_2O_3,
$m_{O,G}$ = mass fraction of oxygen in main gas stream.

In deriving equation (54), the oxygen concentration at the surface of the steel has been

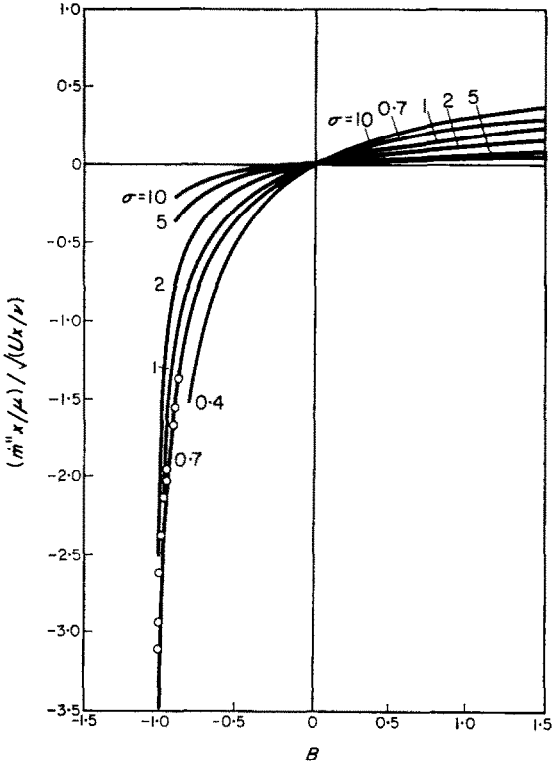

FIG. 19. $(\dot{m}''x/\mu)/\sqrt{(Ux/\nu)}$ vs. B for flat plate and various σ.
——— calculated curves
○ experimental values for combustion of 0·195% C—steel in oxygen stream (from [29]).

taken as zero; this is justifiable when the surface temperature of the steel is high.

Dimensionless mass-transfer rate. For a given value of B, as obtained from (54), we can determine the corresponding value of $(\dot{m}''/\mu)/\sqrt{(Ux/\nu)}$ for $\beta = 0$ and various σ from the graphs of Fig. 19 which have been derived from Figs. 2 and 5 of Paper 3 [23].

Comparison with experimental results. Also plotted in Fig. 19 are points obtained experimentally for the burning of 0·195% C-steel by Wells [29]. This reference gives the rates of steel disappearance (burning rate plus melting rate); we have converted them to our notation of the form: $(\dot{m}''x/\mu)/(Ux/\nu)$ versus B. In the conversion, the heat loss due to radiation and conduction of steel is neglected, and the property values of the stream are obtained from Kaye and Laby [30] at a reference temperature of 770°C which is the mean of the temperature of the main gas stream and the melting point of the steel; σ is taken as 0·7.

It is seen that the agreement between the experiments and the theoretical prediction ($\sigma = 0{\cdot}7$ line in Fig. 19) is good. It should be mentioned that Wells [29] also presented a theoretical analysis of his results which, though in a different and less general form than the present one, made use of similar assumptions and led to the same satisfactory agreement with experiment.

5. CONCLUSIONS

(a) Similar methods to those presented in Paper 1 for the velocity boundary layer have been developed for calculating the rate of mass transfer through laminar steady uniform-property boundary layers when the surface and transferred-substance conditions are uniform.

(b) The recommended method is represented by equation (44); equation (45) is easier to use but somewhat less accurate.

(c) Where checks have been made, agreement between theory and experiment is satisfactory.

(d) It is shown that a commonly made assumption regarding the Chilton–Colburn relation between the surface shear and the surface conductance for heat and mass transfer is considerably in error for the axi-symmetrical and two-dimensional stagnation points.

REFERENCES

1. D. B. SPALDING, Mass transfer through laminar boundary layers—1. The velocity boundary layer, *Int. J. Heat Mass Transfer*, **2**, Nos. 1/2, 15–22 (1960), Referred to in the text as Paper 1.
2. D. B. SPALDING and H. L. EVANS, Mass transfer through laminar boundary layer—2. Auxiliary functions for the velocity boundary layer, *Int. J. Heat Mass Transfer*, **2**, No. 3, 199–221 (1960). Referred to in the text as Paper 2.
3. D. B. SPALDING and H. L. EVANS, Mass transfer through laminar boundary layer—3. Similar solution of the *b*-equation, *Int. J. Heat Mass Transfer*, **2**, No. 4, 314–341 (1960). Referred to in text as Paper 3.
4. D. B. SPALDING, A standard formulation for the convective mass transfer problem, *Int. J. Heat Mass Transfer*, Nos. 2/3, **1**, 192–207 (1960).
5. A. G. SMITH and D. B. SPALDING, Heat transfer in a laminar boundary layer with constant fluid properties and constant wall temperature, *J. Roy. Aero. Soc.*, **62**, 60–64 (1958).
6. E. R. G. ECKERT, Die Berechnung des Warmeübergangs in der laminaren Grenzschicht umströmter Körper, VDI-Forschungsheft 416, 1–24 (1942).
7. R. A. SEBAN, Calculation method for two-dimensional laminar boundary layers with arbitrary free-stream velocity variation and arbitrary wall-temperature variation. University of California, Inst. Eng. Res. Report 2–12 (May 1950).
8. R. M. DRAKE, Calculation method for three-dimensional rotationally symmetrical laminar boundary layers with arbitrary free stream velocity and arbitrary wall temperature variation, *J. Aero. Sci.* **20**, No. 5, 309–316 (1953).
9. M. J. LIGHTHILL, Contribution to the theory of heat transfer through a laminar boundary layer, *Proc. Roy. Soc.* A, **202**, 359–317 (1950).
10. H. SCHUH (1953), A new method for calculating laminar heat transfer on cylinders of arbitrary cross section and on bodies of revolution at constant and variable wall temperature. Roy. Inst. Tech. KTN Aero TN 33, Sweden (1953).
11. H. B. SQUIRE, Heat transfer calculation for aerofoils, Aero Res. Com. Rep. Mem. No. 1986 (1942).
12. D. B. SPALDING, Heat transfer from surfaces of non-uniform temperature, *J. Fluid Mech.* **4**, Part 1, 22–32 (1958).
13. H. A. STINE and K. WANLASS, Theoretical and experimental investigation of aerodynamic heating and isothermal heat transfer parameters on a hemispherical nose with laminar boundary layer at supersonic Mach number. *N.A.C.A.* TN 3344 (1954).
14. D. B. SPALDING and W. M. PUN, A review of methods for predicting heat-transfer coefficients for laminar uniform-property boundary layer flows, *Int. J. Heat Mass Transfer* **5**, No. 2, 239 (1962).

15. E. R. G. ECKERT and J. N. B. LIVINGOOD, Method for calculation of heat transfer in laminar region of air flow around cylinder of arbitrary cross section, *N.A.C.A.* TN 2733 (1952).
16. A. WALZ, Ein neuer Ansatz für Geschwindigkeitsprofil der laminaren Reibungsschicht. *Lilienthal-Bericht* **141**, No. 8 (1941).
17. E. SCHMIDT and K. WENNER, Wärmeabgabe über den Umfang eines angeblasenen geheizten Zylinders, *Forsch. Ing.* **12**, 65–73 (1941).
18. W. MANGLER (1948), Zusammenhang zwischen ebenen und rotationssymmetrischen Grenzschichten kompressiblen Flüssigkeiten, *Z. Angew. Math. Mech.* **28**, 97 (1948)
19. D. B. SPALDING and A. G. SMITH, Verbrennung flüssiger und fester Brennstoffe als Grenzschichtproblem. *Brennstoff-Wärme-Kraft.* **10**, 271–273 (1958).
20. D. B. SPALDING, Experiments on the burning and extinction of liquid fuel spheres, *Fuel, Lond.* **32**, 169–185 (1953).
21. D. B. SPALDING, Heat and mass transfer in aeronautical engineering, *Aero Quarterly*, **11**, 105–136 (1960).
22. D. B. SPALDING, The prediction of mass-transfer rates when equilibrium does not prevail at the phase interface, *Int. J. Heat Mass Transfer*, **2**, 283–313 (1961).
23. D. B. SPALDING, Comment on "Adiabatic wall temperature due to mass transfer cooling with a combustible gas", *J. Amer. Rocket Soc.* **30**, No. 1, 132 (1960).
24. M. C. ADAMS and H. A. BETHE, A theory for the ablation of glassy materials, *J. Aero/Space Sci.* **26**, No. 6, 321–328, 350 (1959).
25. L. LEES, Similarity parameters for surface melting of a blunt body in a high velocity gas stream, *J. Amer. Rocket. Soc.* **29**, 345–354 (1959)
26. T. H. CHILTON and A. P. COLBURN, Mass transfer (absorption) coefficients, *Industr. Engng. Chem.*, **26**, 1183–1187 (1934).
27. N. FRÖSSLING, Evaporation, heat transfer and velocity distribution in two-dimensional and rotational symmetrical laminar boundary-layer flow, *N.A.C.A.* TM 1432 (1958).
28. D. B. SPALDING, *Some Fundamentals of Combustion*, pp. 119–122. Butterworth's Scientific Publication (1955).
29. A. A. WELLS, The iron–oxygen combustion process: A study related to oxygen cutting. *Brit. Welding J.* 392–400 (1955).
30. G. W. C. KAYE and T. H. LABY, *Tables of Physical and Chemical constants and some Mathematical functions*, 12th Ed. Longmans, Green and Co., London (1959).

APPENDIX A

Method of calculation of the F_4 function for $\sigma \to \infty$
(For full explanation of notation, see Paper 3)

When σ tends to infinity, the procedure described in Section 4.4 of Paper 3 may be modified as follows:

(i) Since B remains finite, equation (26) of Paper 3 dictates that f_0 tends to zero as $\sigma \to \infty$.

(ii) The corresponding value of f_0'', obtained from the solutions of the velocity equation given in Paper 2, therefore depends only on β.

(iii) The choice of σ is unnecessary.

(iv) J is now best written as $-B/I$; K is zero by reason of equation (53).

(v) A choice of J now gives a value of I directly from Table 4 of Paper 3.

(vi) Hence such a choice leads to values of

$$\frac{B}{b_0'}\left(\frac{\sigma f_0''}{6}\right)^{1/3}$$

and of B; for the former equals I, from equation (51) of Paper 3, while the latter equals $-IJ$ as just shown.

(vii) Since

$$\sigma^{2/3}\frac{u_G}{\nu}\frac{d\Delta_4^2}{dx} = 2(1-\beta)\left(\frac{B}{b_0'}\right)^2\sigma^{2/3} \qquad \text{(A1)}$$

Table A1. β, f_0'' etc. for $\sigma \to \infty$

β	f_0''	$2(1-\beta)(6/f_0'')^{2/3}$	$\beta(6/f_0'')^{2/3}$
−0·19	0·0860	40·34	−3·220
−0·18	0·1285	30·60	−2·334
−0·16	0·1905	23·14	−1·596
−0·15	0·2161	21·08	−1·375
−0·14	0·2395	19·52	−1·199
−0·10	0·3191	15·56	−0·7071
−0·05	0·4008	12·75	−0·0304
0	0·4696	10·93	0
0·1	0·5870	8·478	0·4710
0·2	0·6869	6·786	0·8483
0·3	0·7748	5·480	1·1743
0·4	0·8542	4·401	1·4671
0·5	0·9277	3·472	1·736
0·6	0·9960	2·649	1·987
0·8	1·1200	1·225	2·449
1·0	1·2326	0	2·873
1·2	1·336	−1·089	3·266
1·4	1·431	−2·080	3·641
1·6	1·521	−2·997	3·996
1·8	1·606	−3·852	4·337
2·0	1·687	−4·660	4·660
2·2	1·764	−5·428	4·976
2·4	1·837	−6·164	5·284

and

$$\sigma^{2/3}\frac{\Delta_4^2}{\nu}\frac{\mathrm{d}u_G}{\mathrm{d}x} = \beta\left(\frac{B}{b_0''}\right)^2\sigma^{2/3} \qquad \text{(A2)}$$

from equations (36) and (35) of Paper 3 respectively, we can write the following relations for the quantities appearing in Table 3 and Fig. 6:

$$F_4\,\sigma^{2/3} = 2(1-\beta)\left(\frac{6}{f_0''}\right)^{2/3} I^2 \qquad \text{(A3)}$$

and

$$\sigma^{2/3}\frac{\Delta_4^2}{\nu}\frac{\mathrm{d}u_G}{\mathrm{d}x} = \beta\left(\frac{6}{f_0''}\right)^{2/3} I_2 \qquad \text{(A4)}$$

where in I is a function only of B and f_0'' is a function only of β.

The last-named functions are contained in Tables A1 and A2. The former is deduced from the $f_0 = 0$ data in Table 1 of Paper 2; the latter is deduced from the $K = 0$ data of Table 3 of Paper 3.

Table A2. J, I, B and I^2 for $\sigma \to \infty$

J	I	$B(=-IJ)$	I^2	J	I	$B(=-IJ)$	I^2
0	0·8930	0	0·7974	0	0·8930	0	0·7974
0·10	0·8495	−0·0850	0·7217	−0·1	0·9398	0·0940	0·8832
0·20	0·8090	−0·1618	0·6545	−0·2	0·9903	0·1981	0·9807
0·30	0·7713	−0·2314	0·5949	−0·3	1·0448	0·3135	1·0916
0·40	0·7362	−0·2945	0·5420	−0·4	1·1037	0·4415	1·2182
0·50	0·7035	−0·3517	0·4949	−0·5	1·1674	0·5837	1·3268
0·60	0·6729	−0·4037	0·4528	−0·6	1·2364	0·7418	1·5287
0·70	0·6443	−0·4510	0·4151	−0·7	1·3112	0·9178	1·7192
0·80	0·6175	−0·4940	0·3813	−0·8	1·3924	1·1139	1·9388
0·90	0·5924	−0·5332	0·3509	−0·9	1·4806	1·3325	2·1922
1·00	0·5688	−0·5689	0·3235	−1·0	1·5766	1·5766	2·4857
1·10	0·5468	−0·6015	0·2990	−1·1	1·6812	1·8494	2·8264
1·20	0·5260	−0·6313	0·2767	−1·2	1·7954	2·1544	3·2235
1·30	0·5065	−0·6585	0·2565	−1·3	1·9200	2·4960	3·6864
1·40	0·4881	−0·6834	0·2382	−1·4	2·0563	2·8788	4·2284
1·50	0·4708	−0·7062	0·2217	−1·5	2·2056	3·3084	4·8647
1·60	0·4544	−0·7271	0·2065	−1·6	2·3692	3·7907	5·6131
1·70	0·4390	−0·7463	0·1927	−1·7	2·5488	4·3330	6·4960
1·80	0·4244	−0·7639	0·1801	−1·8	2·7462	4·9432	7·5416
1·90	0·4106	−0·7801	0·1686	−1·9	2·9635	5·6306	8·7823
2·00	0·3975	−0·7950	0·1581	−2·0	3·2028	6·4057	10·258
2·10	0·3851	−0·8087	0·1483	−2·1	3·4669	7·2805	12·019
2·20	0·3734	−0·8214	0·1394	−2·2	3·7586	8·2690	14·127
2·30	0·3622	−0·8331	0·1319	−2·3	4·0813	9·3869	16·657
2·40	0·3516	−0·8438	0·1236	−2·4	4·4386	10·653	19·701
2·50	0·3415	−0·8538	0·1166	−2·5	4·8348	12·087	23·375
2·60	0·3319	−0·8630	0·1102	−2·6	5·2747	13·714	27·822
2·70	0·3228	−0·8715	0·1042	−2·7	5·7637	15·562	33·220
2·80	0·3141	−0·8794	0·0987	−2·8	6·3079	17·662	39·790
2·90	0·3058	−0·8867	0·0935	−2·9	6·9145	20·052	47·810
3·00	0·2978	−0·8935	0·0887	−3·0	7·5913	22·774	57·628
3·25	0·2795	−0·9084	0·0781	−3·25	9·6536	31·374	93·192
3·50	0·2631	−0·9209	0·0692	−3·50	12·396	43·387	153·67
3·75	0·2484	−0·9314	0·0617	−3·75	16·072	60·270	258·31
4·00	0·2350	−0·9402	0·0552	−4·00	21·036	84·145	442·52
4·25	0·2230	−0·9476	0·0497	4·25	27·792	118·115	772·338
4·50	0·2120	−0·9540	0·0449	−4·50	37·054	166·743	1373·0
4·75	0·2011	−0·9594	0·0404	−4·75	49·848	236·78	2484·8
5·00	0·1928	−0·9641	0·0372	−5·00	67·649	338·25	4576·4

Résumé—Les solutions exactes des équations de la couche limite laminaire à propriétés constantes présentées dans un article précédent sont utilisées pour le développement de méthodes approchées permettant de calculer les coefficients de transport de masse dans le cas de surfaces bidimensionnelles ou de révolution, la vitesse de l'écoulement principal étant arbitraire et les conditions de la matière transportée et de l'interface étant constantes le long de la surface. Le taux de transport de masse est obtenu avec une précision suffisante dans bien des cas, à partir du calcul d'une seule quadrature où figureent la vitesse de l'écoulement principal et des constantes dépendant du nombre de Prandtl/Schmidt; on propose une méthode d'itération pour améliorer un peu la précision. La méthode est un développement de celle d'Eckert et Livingood et fait usage du procédé de quadrature de Walz.

Zusammenfassung—Die exakten Lösungen der laminaren Grenzschichtgleichungen mit einheitlichen Stoffeigenschaften wurden in früheren Arbeiten dieser Reihe angegeben. Hier dienen sie dazu, Näherungsmethoden zur Bestimmung des Stoffüberganges an zweidimensionalen und achssymmetrischen Oberflächen bei beliebiger Hauptstromgeschwindigkeit zu entwickeln, soweit die Stoffeigenschaften der Trennfläche und der übertragenen Substanz entlang der Oberfläche einheitlich bleiben. Die Stoffübergangsgeschwindigkeit lässt sich für viele Zwecke genügend genau durch Auswertung einer einzigen Quadratur erhalten, die die Hauptstromgeschwindigkeit und die von der Prandtl/Schmidtzahl abhängigen Konstanten einschliesst. Mit einem angegebenen Iterationsverfahren lässt sich die Genauigkeit etwas steigern. Die Methode ist nach jener von Eckert und Livingood unter Benützung des Quadraturverfahrens von Walz weiterentwickelt.

Аннотация—Полученные в предыдущих статьях точные решения уравнений ламинарного пограничного слоя с постоянными характеристиками используются для разработки приближенных методов расчета скорости переноса массы с двумерных и осесимметричных поверхностей при произвольной скорости основного потока, постоянных условиях на поверхности раздела и постоянных условиях переноса вещества вдоль поверхности. Для многих случаев скорость переноса массы получена с достаточной точностью одной квадратурой, включающей скорость основного потока и постоянные, зависящие от критерия Прандтля/Шмидта. Проведен повторный расчет, несколько повышающий точность. Данный метод является развитием метода Эккерта и Ливингуда и использует метод квадратур Вольца.